

Oligomer formation during gas-phase ozonolysis of small alkenes and enol ethers: new evidence for the central role of the Criegee Intermediate as oligomer chain unit

A. Sadezky^{1,2}, R. Winterhalter¹, B. Kanawati¹, A. Römpp³, B. Spengler³,
A. Mellouki², G. Le Bras², P. Chaimbault⁴, and G. K. Moortgat¹

¹Max-Planck-Institute for Chemistry, Atmospheric Chemistry Department, P.O. Box 3060,
55020 Mainz, Germany

²Institut de Combustion Aérothermique Réactivité et Environnement, CNRS, 1C Avenue de la
Recherche Scientifique, 45071 Orléans Cedex 2, France

³Institut für Anorganische und Analytische Chemie, Justus-Liebig-Universität, 35392 Giessen,
Germany

⁴Institut de Chimie Organique et Analytique, UMR 6005, BP 6759, Université d'Orléans,
45067 Orléans Cédex 2, France

Received: 6 August 2007 – Accepted: 3 September 2007 – Published: 4 October 2007

Correspondence to: G. K. Moortgat (moo@mpch-mainz.mpg.de)

14041

Abstract

An important fraction of secondary organic aerosol (SOA) formed by atmospheric ox-
idation of diverse volatile organic compounds (VOC) has recently been shown to con-
sist of high-molecular weight oligomeric species. In our previous study (Sadezky et al.,
5 2006), we reported the identification and characterization of oligomers as main con-
stituents of SOA from gas-phase ozonolysis of small enol ethers. These oligomers
contained repeated chain units of the same chemical composition as the main Criegee
Intermediates (CI) formed during the ozonolysis reaction, which were CH_2O_2 (mass
46) for alkyl vinyl ethers (AVE) and $\text{C}_2\text{H}_4\text{O}_2$ (mass 60) for ethyl propenyl ether (EPE).
10 In the present work, we extend our previous study (Sadezky et al., 2006) to another
enol ether (ethyl butenyl ether EBE) and a variety of structurally related small alkenes
(*trans*-3-hexene, *trans*-4-octene and 2,3-dimethyl-2-butene).

Experiments have been carried out in a 570 l spherical glass reactor at atmospheric
conditions in the absence of seed aerosol. SOA formation was measured by a scan-
ning mobility particle sizer (SMPS). SOA filter samples were collected and chemically
15 characterized off-line by ESI(+)/MS-TOF and ESI(+)/MS/MS-TOF, and elemental com-
positions were confirmed by ESI(+)/MS/MS-FTICR. The results for all investigated un-
saturated compounds are in excellent agreement with the observations of our previous
study (Sadezky et al., 2006). Analysis of the collected SOA filter samples reveal the
20 presence of oligomeric compounds in the mass range 200 to 800 u as major con-
stituents. The repeated chain units of these oligomers are shown to systematically
have the same chemical composition as the respective main Criegee Intermediate (CI)
formed during ozonolysis of the unsaturated compounds, which is $\text{C}_3\text{H}_6\text{O}_2$ (mass 74)
for ethyl butenyl ether (EBE), *trans*-3-hexene, and 2,3-dimethyl-2-butene, and $\text{C}_4\text{H}_8\text{O}_2$
25 (mass 88) for *trans*-4-octene. Analogous fragmentation pathways among the oligomers
formed by gas-phase ozonolysis of the different alkenes and enol ethers in our present
and previous study (Sadezky et al., 2006), characterized by successive losses of the
respective CI-like chain unit as a neutral fragment, indicate a similar principal struc-

14042

ture. As in our previous work (Sadezky et al., 2006), we suggest the basic structure of a linear oligoperoxide $[\text{CH}(\text{R})\text{-O-O}]_n$ for all detected oligomers, with the repeated chain unit $\text{CH}(\text{R})\text{OO}$ corresponding to the respective major CI. Furthermore, copolymerization of CI simultaneously formed in the gas phase from two different unsaturated compounds is shown to occur during the ozonolysis of a mixture of *trans*-3-hexene and ethyl vinyl ether (EVE), leading to formation of oligomers with mixed chain units $\text{C}_3\text{H}_6\text{O}_2$ (mass 74) and CH_2O_2 (mass 46). We therefore suggest oligoperoxide formation to be a general, so far unknown reaction pathway of small stabilized CI in the gas phase, which represents an alternative way to high-molecular products and thus contributes to SOA formation.

1 Introduction

Organic material accounts for a substantial fraction of atmospheric fine particulate matter that affects the global climate by direct and indirect effects as well as human health (Pöschl, 2005, and references therein). Secondary organic aerosol (SOA) is formed by gas-to-particle conversion of products of the tropospheric photooxidation of volatile organic compounds (VOC), and its global formation is estimated to range from 12 to 70 Tg y^{-1} (Kanakidou et al., 2005, and references therein). Understanding the chemical composition and formation processes of SOA is required for a quantitative assessment of its production, properties and environmental effects (Fuzzi et al., 2006).

An important fraction of organic aerosol consists of high-molecular weight organic species, as have shown several studies of a wide range of VOC oxidation reactions. Most studies suggest that oligomerization takes place through heterogeneous condensation reactions of more volatile reaction products on the surface and within the bulk of aerosol particles, producing stable oligomeric compounds. Such reactions are aldol condensation and *gem*-diol formation (Gao et al., 2004; Tolocka et al., 2004), acid dehydration (Hamilton et al., 2006; Gao et al., 2004) and esterification (Hamilton et al., 2006; Surratt et al., 2006). Identified monomers were typical low-volatile reaction prod-

14043

ucts formed during gas-phase ozonolysis of cycloalkenes, such as multifunctional acids and diacids (Hamilton et al., 2006; Gao et al., 2004) and 2-methylglyceric acid formed during photooxidation of isoprene in the presence of high NO_x -concentrations (Surratt et al., 2006). Aldol and *gem*-diol condensation reactions have been reported to be significantly enhanced by acidic seed particles providing acid catalysis (Gao et al., 2004; Tolocka et al., 2004). Moreover, oligomer formation was detected during photooxidation of 1,3,5-trimethylbenzene and α -pinene by on-line aerosol time-of-flight (ATOF) mass spectrometry (Gross et al., 2006) and off-line matrix-assisted laser desorption mass spectrometry (Gross et al., 2006; Kalberer et al., 2004). Kalberer et al. (2004) attributed the oligomers observed during photooxidation of 1,3,5-trimethylbenzene to hydration-condensation reactions involving the main reaction products of aromatic photooxidation, glyoxal and methylglyoxal. These condensation processes are described as part of SOA aging processes taking place over several hours after SOA formation.

Furthermore, a variety of high-molecular peroxidic compounds mainly formed as reaction products of stabilized Criegee Intermediates have been identified as important SOA constituents. Among those products are secondary ozonides, α -acyloxyalkyl hydroperoxides, cyclic geminal diperoxides, peroxyhemiacetals and diacyl peroxides (Zahardis and Petrucci, 2007; Mochida et al., 2006; Reynolds et al., 2006; Tolocka et al., 2006; Zahardis et al., 2006, 2005; Docherty et al., 2005; Dreyfus et al., 2005; Ziemann, 2003, 2002). Initial unsaturated compounds are either monoterpenes and cyclic alkenes consisting of six to ten carbon atoms (Tolocka et al., 2006; Docherty et al., 2005; Ziemann, 2003; Ziemann, 2002), cholesterol (Dreyfus et al., 2005) or the linear C18 oleic acid and methyl oleate (Zahardis and Petrucci, 2007; Mochida et al., 2006; Reynolds et al., 2006; Zahardis et al., 2006, 2005). Formation reactions leading to those high-molecular peroxidic compounds were partly suggested to take place in the liquid phase within the aerosol particles or heterogeneously. Furthermore, formation of oligomers from peroxidic reactions products of oleic acid and cholesterol ozonolysis was reported to proceed via their additional free carboxylic acid and carbonyl functionalities, which react with other, eventually multifunctional Criegee Intermediates

14044

(Zahardis and Petrucci, 2007; Zahardis et al., 2006; Reynolds et al., 2006; Dreyfus et al., 2005).

Other suggested pathways leading to oligomer formation in organic atmospheric aerosol involve aqueous-phase reactions of pyruvic acid, a product of the atmospheric oxidation of isoprene, initiated by OH radicals (Altieri et al., 2006) or photolysis (Guzman et al., 2006) within cloud droplets. Recently, formation of higher-molecular weight species was also observed for photooxidation and ozonolysis of tertiary alkylamines (Murphy et al., 2007).

In our recent study (Sadezky et al., 2006) we reported the discovery of oligomeric compounds by chemical analysis of secondary organic aerosol formed during ozonolysis of enol ethers using the off-line ESI/MS-TOF technique. These oligomers were found to consist of repetitive chain units, which have the same elementary compositions as the main Criegee Intermediates (CI) formed from these ozonolysis reactions: CH_2O_2 (= CH_2OO for C_1 -CI) of mass 46 for the alkyl vinyl ethers (AVE) and $\text{C}_2\text{H}_4\text{O}_2$ (= CH_3CHOO for C_2 -CI) of mass 60 for ethyl propenyl ether (EPE). It is proposed that these oligomers have the following basic structure of an oligoperoxide, $-\text{[CH(R)-O-O]}_n-$, where $\text{R} = \text{H}$ for the AVE and $\text{R} = \text{CH}_3$ for the EPE. We suggested a new pathway for secondary organic aerosol and oligomer formation involving gas-phase reactions involving stabilized CI, which lead to formation of oligoperoxidic chains carrying mostly three to four CI-like chain units.

Our present work is aimed at investigating the possibility that the correlation between the structure of the main Criegee Intermediate formed during alkene ozonolysis and the composition of formed SOA and oligomers described in our previous work (Sadezky et al., 2006) might apply to a wider range of unsaturated compounds. We therefore extend our previous study (Sadezky et al., 2006) to a wider variety of small unsaturated compounds, among which are another enol ether, ethyl butenyl ether (EBE, $\text{C}_2\text{H}_5\text{OCH}=\text{CHC}_2\text{H}_5$), and three symmetric hydrocarbon alkenes, *trans*-3-hexene ($\text{C}_2\text{H}_5\text{CH}=\text{CHC}_2\text{H}_5$), 2,3-dimethyl-2-butene ($(\text{CH}_3)_2\text{C}=\text{C}(\text{CH}_3)_2$), and *trans*-4-octene ($\text{C}_3\text{H}_7\text{CH}=\text{CHC}_3\text{H}_7$). A gas-phase ozonolysis experiment of a mixture of

14045

ethyl vinyl ether (EVE, $\text{C}_2\text{H}_5\text{O}-\text{CH}=\text{CH}_2$) and *trans*-3-hexene ($\text{C}_2\text{H}_5\text{CH}=\text{CHC}_2\text{H}_5$) was also performed in order to investigate a possible formation of mixed oligomers that might contain combinations of chain units corresponding to the main CI formed during both reactions. Gas-phase ozonolysis experiments have been performed in a laboratory-reaction chamber under experimental conditions similar to those of Sadezky et al. (2006). SOA formed during the reactions have been observed by a SMPS system and chemically characterized by a hybrid ESI(+)/Q-TOF and chemical composition was confirmed by accurate mass measurements with an ESI Fourier Transform Ion cyclotron resonance (FTICR) mass spectrometer. FTICR MS offers ultrahigh resolution and high sensitivity for the characterization of complex samples (e.g. Römpf et al., 2005).

2 Experimental

Experiments in the laboratory were performed in a 570-liter spherical glass reactor at room temperature in synthetic air at a total pressure of 730 Torr. A detailed description of this setup has been described in earlier publications (Neeb et al., 1998; Winterhalter et al., 2000). Ozone was produced by a mercury pen-ray lamp inside the reactor, prior to the addition of the mixture of the unsaturated compound and synthetic air (reaction start). The concentrations of reactants and reaction products were followed by Fourier Transform infrared spectroscopy (FTIR). The aerosol concentration and size distribution was monitored with a scanning mobility particle sizer (SMPS, TSI 3936) and provides information of the total SOA mass M_0 . The SMPS consists of an electrostatic classifier (TSI 3080) with a long differential mobility analyzer, (LDMA; TSI 3081) and an ultrafine condensation particle counter (CPC; TSI 3025A) as detector.

Experiments were performed with initial ozone mixing ratios of 8 ppm, and enol ether and alkene mixing ratios of 15 ppm. For simultaneous ozonolysis of EVE and *trans*-3-hexene, initial mixing ratios were 8 ppm of ozone, 8 ppm of EVE and 12 ppm of *trans*-3-hexene. In order to prevent reactions of vinyl ethers with OH radicals, which are known

14046

to be generated during the ozonolysis of alkenes (Finlayson et al., 1972), cyclohexane (excess, 300 ppm) was added in some experiments. All chemicals were commercially available (purity >95%) and used without further purification.

The aerosol formed in the laboratory experiments was collected during 20–25 min on Teflon (PTFE) filters (45 mm diameter, 0.45 μm pore size), using a flow rate of 14 L min^{-1} . After collection the filters were extracted in a 7 cm^3 glass flask with 3 ml pure methanol (HPLC grade), and stored at -20°C until analysis.

Chemical constituents were detected by a hybrid mass spectrometer (quadrupole and time-of-flight) QSTAR (Applied Biosystems MDS SCIEX) with an electrospray ion source. The extraction solution was directly injected (30 $\mu\text{l}/\text{min}$). The electrospray ion source (TurbolonSpray) was operated in the positive mode at 400°C and an ionization voltage of +3.4 kV. The declustering potential was 0 to + 30 V, and the focussing potential (focus ring) was + 100 V. For tandem Q-TOF experiments, the collision energy was between 10 and 30 eV with CAD (collision gas) set to 2. Instrument control, spectra treatment and calculations of elemental compositions were done with the software Analyst (Applied Biosystems MDS SCIEX). Moreover, the elemental composition of the analytes was determined by nanoelectrospray Fourier transform ion cyclotron resonance (FTICR) mass spectrometry. The instrument used was a combined linear ion trap and FTICR mass spectrometer (LTQ FT, Thermo Electron, Bremen, Germany). The sample was introduced by a nanospray source using fused-silica emitters (New Objective, Woburn, MA, USA) at an ionization potential of +1 kV. Data analysis was done with the Xcalibur 2.0 software (Thermo Electron, Bremen, Germany). Due to a technical problem the mass accuracy for these measurements was 10 ppm.

14047

3 Results and discussion

3.1 Gas phase reaction mechanisms

3.1.1 Enol ethers

The general mechanism of the ozonolysis of enol ethers is displayed in Fig. 1a. The initial product formed is the primary ozonide (1,2,3-trioxolane), which is unstable and decomposes into a carbonyl oxide, called the Criegee intermediate (CI), and a primary carbonyl compound. The ozonolysis of enol ether molecules produces CIs of the type CH_2OO ($\text{C}_1\text{-CI}$, $\text{R}'=\text{H}$) for the alkyl vinyl ethers (AVE), CH_3CHOO ($\text{C}_2\text{-CI}$, $\text{R}'=\text{CH}_3$) for ethyl propenyl ether (EPE), and $\text{C}_2\text{H}_5\text{CHOO}$ ($\text{C}_3\text{-CI}$, $\text{R}'=\text{C}_2\text{H}_5$) for ethyl butenyl ether, together with ROCHOO (alkoxy-substituted CI).

The corresponding primary carbonyl compounds consist of an alkyl formate ROC(O)H and formaldehyde (AVE, $\text{R}'=\text{H}$), acetaldehyde (EPE, $\text{R}'=\text{CH}_3$) or propanal (EBE, $\text{R}'=\text{C}_2\text{H}_5$).

Previous studies of the gas-phase ozonolyses of ethyl vinyl ether (EVE, $\text{C}_2\text{H}_5\text{O-CH=CH}_2$) and ethyl propenyl ether (EPE, $\text{C}_2\text{H}_5\text{O-CH=CHCH}_3$) by FTIR spectroscopy showed that the branching ratios of the splitting of the primary ozonide into both pathways was $(71\pm 13)\%$ for the “ethyl formate + $\text{C}_1\text{-CI}$ ” channel for EVE, and $(83\pm 13)\%$ for the “ethyl formate + $\text{C}_2\text{-CI}$ ” channel for EPE (Sadezky, 2005). In this work, the branching ratio for the “ethyl formate + $\text{C}_3\text{-CI}$ ” channel during ozonolysis of EBE was also determined to be close to 80%.

3.1.2 Symmetric alkenes

Symmetric alkenes form only one type of primary carbonyl compound and Criegee Intermediate upon their reaction with ozone (Fig. 1b). The symmetric alkene *trans*-3-hexene therefore produces only CIs of the type $\text{C}_2\text{H}_5\text{CHOO}$ ($\text{C}_3\text{-CI}$, $\text{R}'=\text{C}_2\text{H}_5$), which is also the major CI formed during ozonolysis of ethyl butenyl ether (EBE). *Trans*-4-octene

14048

forms the analogous CIs of the type C_3H_7CHOO (C_4 -CI, $R'=C_3H_7$).

The primary carbonyl compounds simultaneously formed are the corresponding aldehydes propanal (*trans*-3-hexene, $R'=C_2H_5$) and butanal (*trans*-4-octene, $R'=C_3H_7$).

5 2,3-Dimethyl-2-butene produces CIs of the type $(CH_3)_2COO$ (*iso*- C_3 -CI), which is an isomer of the C_3 -CI formed from the ozonolyses of *trans*-3-hexene and EBE. The corresponding primary carbonyl compound is acetone.

10 The CI formed from the decomposition of the primary ozonide are formed in excited states, which then either decompose into various products or become collisionally stabilized.

About 50–60% of the excited C_1 -CI are stabilized, while the yields of stabilized C_2 -CI and C_3 -CI are estimated to be between 20 and 40% per reacted alkene or enol ether (Sadezky, 2005; Kroll et al., 2002). The stabilization rate of the excited *iso*- C_3 -CI, however, is very low, as this type of CI decomposes by nearly 100% via the hydroperoxide channel (e.g. Rickard et al., 1999).

3.2 Formation of secondary organic aerosol (SOA)

15 Total SOA masses M_0 ($\mu g/m^3$) measured by SMPS after completion of the reaction, before the beginning of the filter sampling, are given in Table 1. Initial mixing ratios of reactants and of cyclohexane (C_6H_{12}) added as OH scavenger, and the main types of CI formed from these ozonolysis reactions, as discussed in the previous section, are also given.

25 Measured total SOA masses M_0 formed during gas phase ozonolysis amount to several hundreds of $\mu g/m^3$ for most unsaturated compounds, except the 2,3-dimethyl-2-butene, which forms much lower amounts of SOA. The reason for this difference might be the very low stabilization rate (less than 1% of stabilized CI) of the disubstituted *iso*- C_3 -CI in comparison with the monosubstituted C_3 -CI and C_4 -CI (20% to 40% of stabilized CI) (Kroll et al., 2002; Rickard et al., 1999). A correlation between the amount of SOA formed and the stabilization rate of the CI independently of their num-

14049

ber of carbon atoms – as the disubstituted C_3 -CI and the monosubstituted *iso*- C_3 -CI are isomers – might indicate a key role of stabilized CI in SOA formation.

5 A significant increase of the total SOA mass M_0 upon addition of an excess of cyclohexane (C_6H_{12}) as an OH radical scavenger is observed for the two alkenes *trans*-3-hexene and 2,3-dimethyl-2-butene. A similar influence of C_6H_{12} on SOA yields has been observed by Docherty et Ziemann (2003) for the ozonolysis of β -pinene, while the reverse effect was found for the ozonolysis of alkyl vinyl ethers (Sadezky et al., 2006). In all cases, however, the qualitative results obtained from chemical analysis of the SOA by mass spectrometry do not change in the presence of an OH scavenger.

10 3.3 Chemical analysis of the SOA: Identification of oligomers

3.3.1 ESI(+)/MS-TOF

Deploying the smooth ionisation of the electrospray technique, oligomeric products were detected in the SOA filter samples for all compounds studied. Figures 2a–d show the mass spectra of the aerosol samples obtained.

15 The spectra show the presence of ions in the mass range between m/z 200 and 800 for the enol ether EBE and between m/z 200 and 600 for the three alkenes with the typical regular structures of oligomers. The ion peaks could be grouped in series whose ions display regular differences of $\Delta m/z=74$ for ethyl butenyl ether (EBE), *trans*-3-hexene and 2,3-dimethyl-2-butene (Figs. 2a–c), and of $\Delta m/z=88$ for *trans*-4-octene (Fig. 2d). The results are consistent with those from analogous studies (Sadezky et al., 2006; Sadezky, 2005), revealing oligomer ions with regular mass differences of $\Delta m/z=46$ for alkyl vinyl ethers (AVE) and $\Delta m/z=60$ for the ethyl propenyl ether (EPE). The pseudomolecular ions are positively charged of the type $[M+H]^+$, where M is the mass of the molecular species.

25 The different ion series for the various unsaturated ethers are presented in Table 2 and correspond to different types of oligomers designated (a), (b), (B), (C), (D), (E), (F), (G). In order to better distinguish the series, the peaks of the series are identified

14050

by different colours, corresponding to the colours of the peaks of Figs. 2a–d. Ion series observed for ethyl vinyl ether (EVE) and ethyl propenyl ether (EPE) are also given for comparison (Sadezky et al., 2006).

The most intense series observed for each ether is coloured in red, and is assigned as oligomer of type (a). The other observed oligomer series usually appear with much lower intensities and differ from the major oligomer series of type (a) by multiples and sums of $\Delta m/z=16$ and $\Delta m/z=14$. Oligomer series with similar differences of $\Delta m/z$ towards the main oligomer series of type (a) are labelled with similar letters and colours in Table 2 and in Figs. 2a–d for the different alkenes and enol ethers. For example, for most enol ethers and alkenes, oligomer ions of type (b) are observed, coloured in green in Table 2 and Figs. 2a–d. They differ from the series of type (a) ions by an additional $\Delta m/z=16$, possibly corresponding to an oxygen atom. While for *trans*-3-hexene and ethyl vinyl ether (EVE), only oligomers of type (a) and (b) are observed, a variety of other ions series appear for ethyl butenyl ether (EBE), *trans*-4-octene, 2,3-dimethyl-2-butene and ethyl propenyl ether (EPE). Mass differences of these oligomer series towards the oligomers of type (a) are, for example, $\Delta m/z=14$ for oligomers (C) and (D) (with $\Delta m/z$ 14 possibly corresponding to a CH_2 group), $\Delta m/z=42$ for oligomer (B) ($\Delta m/z$ 42 = 3 \times $\Delta m/z$ 14, possibly corresponding to three CH_2 groups), and $\Delta m/z=30$ for oligomer (E) ($\Delta m/z$ 30 = $\Delta m/z$ 14 + $\Delta m/z$ 16, eventually accounting in total for a formaldehyde-like unit CH_2O).

As described in a later section of this work and in our previous study (Sadezky et al., 2006), ESI(+)/MS/MS-TOF experiments allowed to fragment the pseudomolecular ions $[\text{M}+\text{H}]^+$ and thus to determine the minimum number n of chain units 46, 60, 74 or 88 contained in the molecular species. In Figs. 2a–d, n are given for the pseudomolecular ions $[\text{M}+\text{H}]^+$ of the most intensive oligomer series designated as type (a). Ions of type (a) and ions of weaker oligomer series suggested to carry similar numbers of chain units, are arranged in vertical columns in Table 2.

Some ions between m/z 150 and 300, which are also observed as fragment ions in the MS/MS spectra (Sect. 3.3.2) of parent oligomer ions, are listed separately on

14051

Figs. 2a–d.

Oligomer ions observed for EBE in the present work corroborate the dependence of their chain unit on the vinylic side =CHR' of the double bond of the initial enol ether derived from the analogous study of AVE and EPE (Sadezky et al., 2006). The schematic structure of an enol ether shown in Fig. 3 displays the two alkyl substituents, R' on the vinylic side =CHR' of the double bond and R on its enolic side =CHOR.

$\text{R}'=\text{C}_2\text{H}_5$ for EBE ($\text{C}_2\text{H}_5\text{OCH}=\text{CHC}_2\text{H}_5$), while $\text{R}'=\text{H}$ for AVE ($\text{ROCH}=\text{CH}_2$) and $\text{R}'=\text{CH}_3$ for EPE ($\text{C}_2\text{H}_5\text{OCH}=\text{CHCH}_3$). R' differs thus by mass 14 (CH_2) between the AVE and EPE as well as between EPE and EBE, a difference that is reflected in the masses of the observed oligomer chain units, which are of $\Delta m/z=46$ for the AVE, $\Delta m/z=60=46 + 14$ for EPE and $\Delta m/z=74=60 + 14$ for EBE.

As discussed in the Sect. 3.1.1, the major Criegee Intermediate (CI) formed with yields around 80% during enol ether ozonolysis originates from the vinylic side of the enol ethers, thus carrying R' as substituent. The major CI produced from EBE is therefore the $\text{C}_3\text{-CI}$ with $\text{R}'=\text{C}_2\text{H}_5$, which is identical to the $\text{C}_3\text{-CI}$ formed during ozonolysis of *trans*-3-hexene (Sect. 3.1.2). The results given in Figs. 2a and b and in Table 2 show that the oligomers obtained from ozonolysis of EBE and *trans*-3-hexene consist of chain units with identical mass 74. Moreover, chain units with similar mass 74 are also found for oligomers formed from 2,3-dimethyl-2-butene (Fig. 2c and Table 2), which produce the *iso*- $\text{C}_3\text{-CI}$, an isomer of the $\text{C}_3\text{-CI}$. Finally, *trans*-4-octene forms the $\text{C}_4\text{-CI}$, which differs by a CH_2 group of mass 14 from the $\text{C}_3\text{-CI}$ produced by EBE and *trans*-3-hexene. The chain units of the oligomers obtained from ozonolysis of *trans*-4-octene (Fig. 2d and Table 2) reflect this difference by their $\Delta m/z=88=74+14$. These results point towards a decisive role of the CI in the formation of the oligomers observed as chemical constituents of the SOA from the different unsaturated compounds.

In our previous study, Sadezky et al. (2006) suggested furthermore that the alkoxy group OR on the enolic side of the initial ether is contained once in each oligomer ion. A comparison of the initial structures of EBE and *trans*-3-hexene shows that each symmetric side of the double bond of *trans*-3-hexene is identical to the vinylic side of

14052

EBE. The enolic side of EBE differs from the vinylic side only by the enolic O atom directly linked to the double bond. Indeed, the oligomer ions of types (a) and (b) from ozonolysis of EBE carry an additional $\Delta m/z$ 16 in comparison with those formed from *trans*-3-hexene (Table 2 and Figs. 2a and b), which might account for once the enolic O atom of EBE. Moreover, Table 2 and Figs. 2a and c show that *trans*-3-hexene and 2,3-dimethyl-2-butene form oligomer ions of type (a) and (b) with identical m/z . Both alkenes, like their Cl, are isomers, carrying the same number of carbon and hydrogen atoms as alkyl substituents on each side of their double bonds.

The results presented in Table 2 and in Figs. 2a–d furthermore show that the degree of oligomerization decreases with increasing size of the chain unit. For the most abundant oligomers, $n=3$ with the chain units of mass 46 (AVE) and mass 60 (EPE) (Sadezky et al., 2006), while $n=2$ with the chain unit of mass 74 (EBE and *trans*-3-hexene, Figs. 2a and b), and $n=1$ with the largest chain unit of mass 88 (*trans*-4-octene, Fig. 2d).

Although the chain units are of similar mass 74, lower degrees of oligomerization are observed for oligomers formed from 2,3-dimethyl-2-butene, with $n=1$ for the most abundant oligomer molecule (Fig. 2c), than for those produced from EBE and *trans*-3-hexene. This observation is consistent with the low total SOA masses formed during ozonolysis of this compound, and might be correlated with the low stabilization rate of the *iso*-C₃-Cl in comparison with the C₃-Cl, eventually leading to a lower fraction of Cl undergoing oligomerization reactions.

3.3.2 ESI(+)/MS/MS-TOF

The fragmentation of the pseudomolecular ions using the MS/MS mode confirms that they consist of an oligomeric structure with the chain unit of $\Delta m/z=74$ (ozonolysis of EBE, *trans*-3-hexene and 2,3-dimethyl-2-butene) and $\Delta m/z=88$ (ozonolysis of *trans*-4-octene). Examples of the MS/MS spectra are displayed in Figs. 4a–d, which show the fragmentation of a selected specific pseudo-molecular ion of the type (a) oligomer from each of the four unsaturated compounds studied. The elemental compositions given for

14053

the ions and neutrals in Figs. 4a–d were confirmed by accurate ESI(+)/MS/MS-FTICR measurements.

Fragmentation pathways of oligomer ions

The main fragment ions observed in the MS/MS spectra can be classified as being part of fragmentation pathways, formed by successive losses of the chain unit as neutral mass 74 or 88, respectively. Two fragmentation pathways, marked in violet and red colour in Figs. 4a–d, can be identified for the type (a) oligomers from all unsaturated compounds. Two more pathways, marked in dark and light green colour, are observed for 2,3-dimethyl-2-butene (Fig. 4c) only.

The results are consistent with MS/MS spectra of oligomer ions produced from gas phase ozonolysis of AVE and of EPE, which are presented in our previous study (Sadezky et al., 2006). They show similar fragmentation pathways consisting of successive losses of the chain units 46 for AVE and 60 for EPE, corresponding to the respective oligomer chain unit. However, in comparison with oligomers formed from the unsaturated compounds investigated in the present work, fragmentation spectra of oligomers formed from AVE or EPE are much more rich and complex, with up to nine fragmentation pathways being simultaneously observed for a parent oligomer ion of type (a) (Sadezky et al., 2006).

Figure 5a–c schematically displays the main fragmentation pathways identified for type (a) oligomer ions from the three enol ethers EBE (C₂H₅OCH=CHC₂H₅) (Fig. 4b), EVE (C₂H₅OCH=CH₂) and EPE (C₂H₅OCH=CHCH₃) (Sadezky et al., 2006). Fragmentation pathways of oligomers from different enol ethers, which show apparent analogies among each other, are marked by similar colours, that is, violet, red or dark green. Thus, two fragmentation pathways, marked in violet and red, are identified for type (a) oligomers from all three enol ethers, while a third pathway, marked in dark green, is observed for EVE and EPE only (Sadezky et al., 2006).

Each fragmentation pathway is initiated by loss of a specific neutral from the pseudomolecular ion, followed by successive fragmentations of neutrals corresponding to

14054

the chain units of masses 46 (EVE), 60 (EPE) or 74 (EBE), respectively. Figures 5a–c shows that fragmentation pathways marked in similar colours terminate by fragment ions of similar m/z . Thus, for all three enol ethers, the fragmentation pathways marked in red and violet colours terminate on fragment ions of m/z 85 and m/z 127, respectively. For EBE, the fragment ion 127 itself is not observed in the MS/MS spectrum of the oligomer (a) parent ion (Fig. 4b), but is deduced by subtraction of mass 74 from the next higher observed fragment ion 201 of the violet-marked pathway. A third pathway, marked in dark green colour and observed for EVE and EPE only, terminates on a fragment ion of m/z 99.

For all fragmentation pathways, the mass of the neutral species initially fragmented from the pseudomolecular ion increases by $\Delta m/z=28$ (possibly corresponding to twice a CH_2 group) between EVE and EPE, as well as between EPE and EBE. Simultaneously, the masses of the respective oligomer chain units increase by $\Delta m/z=14$ (CH_2) with the substituents R' of the initial enol ethers and major CI (Figs. 1 and 3) comprising an additional CH_2 group.

The main fragmentation pathways identified in the MS/MS spectra of type (a) oligomer ions formed from ozonolysis of symmetric alkenes (Figs. 4a, c and d) are schematically depicted in Figs. 6a–c. Representations in similar colours signify apparently analogous fragmentation pathways of type (a) oligomers from different alkenes (Figs. 6a–c) and enol ethers (Fig. 5a–c).

Like for EBE (Fig. 5c), type (a) oligomer ions formed from *trans*-3-hexene and *trans*-4-octene (Figs. 6a and c), show only two main fragmentation pathways marked in violet and red colour. The red-coloured fragmentation pathway terminates for all alkenes and enol ethers in Figs. 5 and 6 on a fragment ion of similar m/z 85. Moreover, for type (a) oligomers from both EBE and *trans*-3-hexene, with similar chain units of mass 74, all fragment ions of the red-marked fragmentation pathways are of identical m/z .

Each fragmentation pathway differs between *trans*-3-hexene and *trans*-4-octene in a similar way as it does between EVE and EPE as well as between EPE and EBE, with the masses of the respective CI and oligomer chain units differing at the same

14055

time by $\Delta m/z=14$ (CH_2 group). Thus, for the violet-coloured fragmentation pathway, the mass of the initially fragmented neutral species increases by $\Delta m/z=28$ (possibly corresponding to twice a CH_2 group) from mass 120 (*trans*-3-hexene) to mass 148 (*trans*-4-octene).

The neutral species whose fragmentation from the pseudomolecular ions initiates the red-marked fragmentation pathways is of mass 162 for EBE and of mass 146 for *trans*-3-hexene. It carries thus an additional $\Delta m/z$ 16 for EBE, which might represent the enolic oxygen atom that causes a similar difference between the pseudomolecular ions from EBE and *trans*-3-hexene themselves (Sect. 3.3.1). Fragment ions of the violet-marked fragmentation pathways differ by $m/z=16$ between *trans*-3-hexene and EBE, indicating that the enolic oxygen, which is additionally contained in the pseudomolecular ions formed from EBE, remains in the fragment ions. The neutral species initially fragmented from the pseudomolecular ions for the violet-marked fragmentation pathways are for both EBE and *trans*-3-hexene of similar mass 120.

MS/MS spectra of type (a) oligomers formed from 2,3-dimethyl-2-butene (Figs. 4c and 6b) show two fragmentation pathways, marked in red and violet colours, which are identical to those described for *trans*-3-hexene. However, in comparison with type (a) oligomers formed from *trans*-3-hexene, those from 2,3-dimethyl-2-butene show additional fragmentation pathways (Figs. 6a and b): one of these pathways, marked in dark green colour, shows analogies with a third fragmentation pathway identified for type (a) oligomers from enol ethers (Fig. 5), which is observed for EVE and EPE, but not for EBE. This fragmentation pathway terminates on fragment ions of identical m/z 99 for EVE, EPE and 2,3-dimethyl-2-butene, and its fragment ions generally differ by $\Delta m/z$ 14 from those of the red-marked fragmentation pathway of the same parent ion. A fourth pathway, marked in light green colour, is observed for the parent oligomer ions from 2,3-dimethyl-2-butene, with its fragment ions differing by $\Delta m/z$ 14 from those of the violet-marked fragmentation pathway.

14056

Elemental compositions

Elemental compositions of parent ions, fragment ions and fragmented neutral molecules given in Figs. 4, 5 and 6 are determined from the measured accurate m/z values during ESI(+)/MS/MS-FTICR experiments. The most suitable candidates are selected by comparison of the measured accurate masses with the calculated exact masses of elemental formulas. Detailed calculations for the red-coloured fragmentation of the pseudomolecular ion 379 formed from *trans*-3-hexene (Figs. 4a and 6a) are given in Table 3a. Tables 3b–d show the calculations for the violet-coloured fragmentation pathways of ion 395 formed from EBE (Figs. 4b and 5c), 379 formed from 2,3-dimethyl-2-butene (Figs. 4c and 6b), and 449 formed from *trans*-4-octene (Figs. 4d and 6c).

Figures 4, 5 and 6 and Tables 3a–d show that the calculated elemental compositions are consistent among parent ions, fragment ions and fragmented neutral molecules that are part of the identified fragmentation pathways of the same oligomer ions. They are moreover in agreement with the suggested analogies between fragmentation pathways of oligomer ions formed from the different alkenes and enol ethers.

Measured accurate m/z values allow a rather doubtless determination of the elemental compositions of the chain units. Analysis of the calculated mass errors in Tables 3a–c show a strong and systematic preference of the elemental composition $C_3H_6O_2$ (calculated exact mass 74.0367 u) for the chain unit of mass 74. The other elemental compositions for mass 74 which might make chemical sense as neutral molecules in order to represent the chain units, $C_4H_{10}O$ and $C_2H_2O_3$, usually show much larger mass errors. Similarly, accurate mass measurements yield the elemental composition $C_4H_8O_2$ (exact mass 88.0524 u) for the chain unit of mass 88 of oligomers formed from *trans*-4-octene (Table 3d). Analogous elemental compositions of CH_2O_2 (exact mass 46.0055 u) for the chain unit 46 and $C_2H_4O_2$ (exact mass 60.0211 u) for the chain unit 60 for oligomers formed from AVE and EPE were found in our previous study (Sadezky et al., 2006).

14057

Further work is needed to elucidate the detailed structures of parent and fragment ions. For their chemical compositions, the elements C, H and O and a single positive charge are taken into account. The fact that good fragmentation spectra are obtained from pseudomolecular ions during MS/MS experiments disagrees with Na^+ adducts.

5 Principal structure of type (a) oligomers

Figures 4, 5 and 6 show that the fragmentation pathways characterized by the regular loss of the chain unit typically range from $m/z = 300$ to 400, the masses of the pseudomolecular ions, down to m/z about 100 for the smallest fragment ions. The regularity of the fragmentation pathways and their analogy for oligomers observed from different enol ethers and alkenes indicate that all type (a) oligomers follow the same structural principle. These observations confirm the general linear oligomeric structure that we suggested in our previous work (Sadezky et al., 2006) for type (a) oligomers from the ozonolysis of AVE and EPE. This structure can schematically be represented by a chain having a starting group "X" and an end group "Y" linked by several chain units of mass 46 (AVE), 60 (EPE), 74 (EBE, *trans*-3-hexene and 2,3-dimethyl-2-butene), or 88 (*trans*-4-octene).

An oligomer that contains n chain units of mass 74 is thus represented as $X-(74)_n-Y$. Ionization by ESI(+) leads to the formation of the oligomer pseudomolecular ion $[X-(74)_n-Y+H]^+$. Thus, with $n=2$, this schematic structure might for example represent the pseudomolecular ions 395 (EBE) or 379 (*trans*-3-hexene).

The fragmentation initiates with a loss of a neutral species X or Y from one side of the pseudomolecular ion $[X-(74)_n-Y+H]^+$, leading to the fragment ion $[X-(74)_n+H]^+$ or $[Y-(74)_n+H]^+$. Considering the pseudomolecular ions 395 (EBE) and 379 (*trans*-3-hexene), X or Y are thus represented by the neutrals initially fragmented, which are of mass 120 for the violet-coloured pathway and of masses 146 (*trans*-3-hexene) and 162 (EBE) for the red-marked pathway. Fragmentation continues with n successive losses of a chain unit of mass 74, to finally terminate on a fragment ion XH^+ or YH^+ that represents the opposite side of the oligomer molecule. Considering the red-coloured frag-

14058

mentation pathway of the pseudo-molecular ions 395 (EBE) and 379 (*trans*-3-hexene), XH^+ or YH^+ is represented by the terminating fragment ions of m/z 85. Regarding the violet-coloured fragmentation pathway, the lowest fragment ions observed in the MS/MS spectra are of m/z 201 (EBE) and of m/z 185 (*trans*-3-hexene) and are not attributed to XH^+ or YH^+ , but to the next higher fragment ion $[X-(74)+H]^+$ or $[Y-(74)+H]^+$.

The neutral species whose fragmentation from the pseudomolecular ions initiates the red-marked fragmentation pathways is of mass 162 for EBE and of mass 146 for *trans*-3-hexene. It carries thus an additional $\Delta m/z$ 16 for EBE, which might represent the enolic oxygen atom that causes a similar difference between the pseudomolecular ions from EBE and *trans*-3-hexene themselves (Sect. 3.3.1). Fragment ions of the violet-marked fragmentation pathways differ by $m/z=16$ between *trans*-3-hexene and EBE, indicating that the enolic oxygen, which is additionally contained in the pseudomolecular ions formed from EBE, remains in the fragment ions. The neutral species initially fragmented from the pseudomolecular ions for the violet-marked fragmentation pathways are for both EBE and *trans*-3-hexene of similar mass 120.

The number of successive losses of the chain unit as a neutral molecule, which are directly observed in the MS/MS spectra, corresponds to the minimum number of chain units n comprised in the oligomer molecule. Values of n are given in Table 2 and in Figs. 2a–d.

In the given schematic representations, the proton ionizing the oligomer molecule is suggested to remain attached to the fragment ions. However, this is an arbitrary decision for illustration purposes, as the determination of the exact fragmentation mechanism needs further investigation.

Isomers

The MS/MS spectra of the type (a) oligomer ions formed from the unsaturated compounds studied in the present work are much less complex than those described for the enol ethers AVE and EPE in our previous study (Sadezky et al., 2006). While between two and four fragmentation pathways are observed for each type (a) oligomer parent

14059

ion in the present work, up to nine fragmentation pathways were simultaneously identified for each parent oligomer ion formed from AVE and EPE. In our previous study by Sadezky et al. (2006), we attributed the richness and complexity of the fragmentation spectra for AVE and EPE to the existence of several isomers of the linear type (a) oligomer parent ion. Therefore, in the MS/MS spectrum of a pseudomolecular ion of a certain m/z , the fragmentation pathways of all its isomers appear simultaneously, leading to the observed large number of different fragmentation pathways.

The much smaller number of fragmentation pathways observed in the present work therefore indicates that a much smaller variety of isomers exists for these oligomer parent ions. The reason of this might be the larger size of the oligomer chain units, which are of mass 74 ($C_3H_6O_2$ for EBE, *trans*-3-hexene and 2,3-dimethyl-2-butene) and mass 88 ($C_4H_8O_2$ for *trans*-4-octene) in the present work compared to mass 46 (CH_2O_2 for AVE) and mass 60 ($C_2H_4O_2$ for EPE) in our previous study (Sadezky et al., 2006). With increasing size, the chain units eventually become more sterically hindered, an effect that might exclude the formation of some isomers and moreover reduce the total degree of oligomerization (Sect. 3.3.1).

Interestingly, MS/MS spectra of type (a) oligomers formed from 2,3-dimethyl-2-butene show at least four different fragmentation pathways (Figs. 4c and 6b), while those of type (a) oligomers from both EBE and *trans*-3-hexene (Figs. 4a and b, 5c and 6a) contain only two fragmentation pathways, marked in red and violet colours. However, the chain units of oligomers from all three compounds are of similar mass 74 and chemical composition $C_3H_6O_2$. A main difference between the compounds is in the structures of their CI: 2,3-dimethyl-2-butene leads to formation of the *iso*- C_3 -CI ($(CH_3)_2COO$), while the major CI produced by both EBE and *trans*-3-hexene is the C_3 -CI (C_2H_5CHOO). When we assume that the oligomer chain units 74 ($C_3H_6O_2$) from EBE and *trans*-3-hexene and those from 2,3-dimethyl-2-butene are isomers in the same way as the respective CI formed during the ozonolysis reaction, then the chain unit that is substituted, like the *iso*- C_3 -CI, by two CH_3 groups is expected to be more compact and therefore less sterically hindered than the chain unit that is substituted,

14060

like the C₃-CI, by a linear alkylic chain R' = C₂H₅.

Therefore, oligomers with chain units of mass 74 substituted corresponding to the *iso*-C₃-CI might be able to form a wider variety of isomers than those with chain units of similar mass 74 that are substituted corresponding to the C₃-CI. For example, the fragmentation pathway marked in dark green colour (Figs. 4, 5, and 6), which generally terminates on fragment ions of *m/z* 99, is observed for the type (a) oligomer ions formed from 2,3-dimethyl-2-butene (*iso*-C₃-CI, (CH₃)₂COO) (Figs. 4c and 6b), but not for those from EBE and *trans*-3-hexene (C₃-CI, C₂H₅CHOO). Furthermore, an analogous fragmentation pathway is observed for type (a) oligomers formed from AVE (C₁-CI, CH₂OO) (Fig. 5a) and EPE (C₂-CI, CH₃CHOO) (Fig. 5b), but not for those from *trans*-4-octene (C₄-CI, C₃H₇CHOO) (Figs. 4d and 6c). Assuming that the oligomer chain units are generally substituted in a similar way as the respective major CI, chain units from EBE, *trans*-3-hexene and *trans*-4-octene supposedly comprise a linear alkyl substituent R' = C₂H₅ (EBE and *trans*-3-hexene) or R' = C₃H₇ (*trans*-4-octene). Chain units from 2,3-dimethyl-2-butene, AVE and EPE, however, carry only CH₃ substituents (2,3-dimethyl-2-butene and EPE) or are not at all substituted (AVE). The dark green-coloured fragmentation pathway might thus originate from an isomer of the pseudo-molecular ion, which is formed only for small chain units similar to the *iso*-C₃-CI or less bulky (C₁-CI, C₂-CI), but might not be stable for sterical reasons for chain units comprising a linear alkyl substituent with two or more CH₂ groups (C₃-CI, C₄-CI).

3.3.3 Oligoperoxidic structure and role of CI for oligomer formation

These results corroborate the decisive role of the Criegee Intermediates in the formation of oligomers, which was already suggested in our previous study (Sadezky et al., 2006). Indeed, the linking chain units of the different oligomers repeatedly have the same elementary compositions as the Criegee Intermediates CI (see Sect. 3.3.2): CH₂O₂ (= CH₂OO for C₁-CI) of mass 46 (AVE), C₂H₄O₂ (= CH₃CHOO for C₂-CI) of mass 60 (EPE), C₃H₆O₂ (= C₂H₅CHOO for C₃-CI or (CH₃)₂COO for *iso*-C₃-CI) of mass 74 (C₃-CI: EBE and *trans*-3-hexene; *iso*-C₃-CI: 2,3-dimethyl-2-butene) and C₄H₈O₂

14061

(=C₃H₇CHOO for C₄-CI) of mass 88 (*trans*-4-octene). In our previous study (Sadezky et al., 2006), we suggested the basic structure of an oligoperoxide for the oligomers identified from ozonolysis of the enol ethers AVE and EPE. We extend this suggestion now to the oligomers formed from the diverse unsaturated compounds studied in the present work, as shown in Fig. 7.

Oligomers with suggested similar structures are known so far only from liquid-phase ozonolysis reactions (Barton et al., 2005, 2004; Lockley et al., 2001; and references therein). Barton et al. (2004) identified by ESI/MS oligoperoxides with *m/z* up to 900 u as reaction products from liquid-phase ozonolysis of 2,3-dimethyl-2-butene ("tetramethyl ethylene" TME) in pentane as a nonparticipating solvent at -60°C. The peroxidic chain link of the mass peaks was of mass 74 and thus corresponded to the CI formed during ozonolysis of 2,3-dimethyl-2-butene, referred to as acetone carbonyl oxide by the authors and as *iso*-C₃-CI (CH₃)₂COO in this work. The authors observed up to 12 chain units for different oligoperoxides. These observations are in excellent agreement with our results for ozonolysis reactions of enol ethers and small alkenes in the gas phase described in the present work and in our previous study (Sadezky et al., 2006). By similar experimental methods, Barton et al. (2005) characterized oligoperoxides formed from the liquid-phase ozonolysis of 3-methyl-2-pentene, which consisted of units of the major CI, referred to as butanone carbonyl oxide (C₄-CI, C₃H₇CHOO, mass 88), randomly copolymerized with units of the corresponding primary carbonyl compound, acetaldehyde (mass 44). The observations of oligomeric peroxides composed of CI-like chain units are again in very good agreement with our studies and with Barton et al. (2004). However, a random incorporation of the corresponding primary aldehydes into those oligomer chains, as was observed by Barton et al. (2005), could not be confirmed in our experiments.

For gas-phase ozonolysis, various mechanisms involving secondary reactions of Criegee Intermediates have been discussed in the literature as formation pathways of major SOA constituents. Unimolecular decomposition of Criegee Intermediates via the "hydroperoxide" and the "hot acid" channel has been suggested as an important

14062

pathway to form low-volatile carboxylic acids, diacids, and peroxidic compounds, such as diacylperoxides, peracids and other multifunctional hydroperoxides, during reactions with ozone of cyclic monoterpenes and cycloalkenes consisting of at least six carbon atoms (Tolocka et al., 2006; Docherty et al., 2005; Keywood et al., 2004; Ziemann, 2002; Koch et al., 2000). Moreover, reactions of stabilized Criegee Intermediates lead to a wide variety of products containing peroxide moieties, several of which were identified in the past as SOA constituents from alkene ozonolysis. The most important reactions among them are those of the stabilized CI with carbonyl compounds to form secondary ozonides and with hydroxylic functionalities of carboxylic acids, alcohols and water to form α -acyloxyalkyl hydroperoxides, α -alkyloxyalkyl hydroperoxides and α -hydroxyalkyl hydroperoxides, respectively. Such products were particularly identified in SOA from ozonolysis reactions of large linear alkenes, such as 1-tetradecene, oleic acid and methyl oleate (Zahardis and Petrucci, 2007, and references therein; Tobias et al., 2000; Tobias and Ziemann, 2000). The presence of secondary ozonides and α -alkyloxyalkyl hydroperoxides has also been reported in SOA formed from cyclic monoterpenes and cycloalkenes containing six to ten carbon atoms (Tolocka et al., 2006; Ziemann, 2003). Some of the peroxidic products have been observed to undergo further association reactions with other molecules in order to form high-molecular weight compounds either in the liquid phase within the SOA particles or heterogeneously on the particle surface. Thus, hydroperoxides formed either by unimolecular decomposition of CI or by reactions of stabilized CI have been observed to react with a variety of aldehydes to form peroxyhemiacetals (Zahardis and Petrucci, 2007, and references therein; Docherty et al., 2005, and references therein). Moreover, peroxidic products in the oleic acid/ozone and cholesterol/ozone reaction systems might carry additional free hydroxyl, carbonyl, or carboxylic acid functionalities, which can further react with other stabilized Criegee Intermediates to form oligomeric compounds (Zahardis and Petrucci, 2007; Zahardis et al., 2006; Dreyfus et al., 2005).

However, none of the above-described mechanisms is consistent with the formation of oligomers with m/z 200 to 800 and repeated CI-like chain units identified as main

14063

SOA constituents in our experiments. Key species of the mechanisms suggested to lead to SOA formation by unimolecular decomposition of CI are acyl radicals, whose structures are based on the original CI formed from cyclic alkenes and monoterpenes and therefore consist of at least five to six C atoms with additional carbonyl or hydroxy functionalities. These acyl radicals are first transformed into acylperoxy radicals by addition of O_2 , which then either react with HO_2 and RO_2 to form low-volatile acids, diacids, peracids and other peroxides (Docherty et al., 2005; Keywood et al., 2004) or cross-react to form diacylperoxides (Ziemann, 2002). However, for the small linear alkenes and enol ethers investigated in this work and in our previous study (Sadezky et al., 2006), the same mechanisms of unimolecular CI decomposition only lead to acyl radicals of the type $R'CO$, with $R'=H, CH_3, C_2H_5, \text{ or } C_3H_7$. By further reaction with O_2, HO_2 and RO_2 , the acyl radicals $R'CO$ form mainly volatile products consisting of four or less C atoms or immediately decompose, while their recombination by cross-reaction (Ziemann, 2002) leads to dimers only and cannot explain the origin of the observed oligomeric chains.

Similarly, peroxidic SOA constituents formed by reactions of the stabilized CI, such as secondary ozonides, α -acyloxyalkyl hydroperoxides and α -alkyloxyalkyl hydroperoxides, involve CI that consist of nine, ten or 13 carbon atoms for the ozonolysis of linear alkenes such as oleic acid (Zahardis and Petrucci, 2007), methyl oleate (Mochida et al., 2006), and 1-tetradecene (Tobias et al., 2000; Tobias and Ziemann, 2000), and of six to ten carbon atoms for cyclic alkenes (Ziemann, 2003) and the monoterpene α -pinene (Tolocka et al., 2006). By their secondary reactions, these stabilized CI often become associated to aldehydes or carboxylic acids of similar sizes, such as nonanoic acid (oleic acid/ozone system, Zahardis and Petrucci, 2007; Zahardis et al., 2006), tridecanal (1-tetradecene ozonolysis, Tobias et al., 2000), or pinonaldehyde (α -pinene ozonolysis, Tolocka et al., 2006), leading to large, low-volatile peroxidic compounds consisting of 18 and more carbon atoms. However, the CI formed from the small unsaturated compounds investigated in our present work and in our previous study (Sadezky et al., 2006) consist of one to four carbon atoms only. Known gas-phase reaction path-

14064

ways following ozonolysis do not lead to larger carbonyl, carboxylic or hydroxylic products either. Therefore, analogous peroxidic products of reactions of the stabilized CI with aldehydes and carboxylic acids formed in the alkene/ozone reaction system are mainly expected to be volatile. Peroxyhemiacetals formed by subsequent reaction of these compounds with aldehydes within the same reaction system, as described by Zahardis and Petrucci (2007), and references therein, and by Docherty et al. (2005), and references therein, do not account for the observed oligomers with regular CI-like peroxidic chain units either. Moreover, oligomerization of these reaction products by mechanisms similar to those described for the oleic acid/ozone reaction by Zahardis and Petrucci (2007) and Zahardis et al. (2006) should be very limited for the ozonolysis of the compounds studied in our work. These mechanisms require the presence of free carbonyl or hydroxylic functionalities on the peroxidic products, which might allow them to further react with other stabilized CI. However, the CI incorporated into the oligomeric molecules carry hydrogen atoms and alkyl groups, with $R'=H$, CH_3 , C_2H_5 , or C_3H_7 . Given the linearity, small sizes and simple structures of the original unsaturated compounds, the main carbonyl, carboxylic and hydroxylic products formed in the reaction system also comprise a single functionality and a non-reactive group derived from R' (or from OR for the enol ethers) rather than being multifunctional. Therefore, oligomerization mechanisms based on the participation of additional reactive functional groups on R' (or OR) cannot explain the observed formation of oligomeric chains consisting of CI-like units in our present work.

Still there is mechanistic evidence that the chemistry of stabilized CI plays a decisive role in oligomer and SOA formation in our reaction system. CI formed from the ozonolysis of small simple alkenes in the gas phase and stabilized by collision with inert gas molecules have been shown to undergo a variety of reactions similar to those known since a long time from liquid-phase chemistry (Calvert et al., 2000, and references therein; Bunnelle, 1991). Reactions of the stabilized C_1 -CI and C_2 -CI have been thoroughly investigated for gas-phase ozonolysis of alkyl vinyl ethers (AVE) and ethyl propenyl ether (EPE) (Sadezky, 2005), ethene (Neeb et al., 1998, 1997), 2-butene

14065

(Horie et al., 1997) and propene (Neeb et al., 1996). A variety of peroxidic products analogous to those described above for larger linear alkenes were identified in these studies: thus, the stabilized C_1 -CI and C_2 -CI react with formaldehyde and acetaldehyde to form secondary ozonides and with the hydroxylic functionalities of water and formic acid to produce the hydroperoxides hydroxymethyl and hydroxyethyl hydroperoxide, as well as hydroperoxymethyl and hydroperoxyethyl formate, respectively. All these products are however highly volatile due to their low molecular weights and were identified only in the gas phase of the alkene/ozone reaction systems. We reported in our previous studies (Sadezky et al., 2006; Sadezky, 2005) that SOA yields from ozonolysis of ethyl vinyl ether (EVE) and ethyl propenyl ether (EPE) were drastically reduced, eventually suppressed, in the presence of an excess of gaseous HCOOH. Simultaneously, oligomers were not detected onto the filter samples taken from these experiments (Sadezky et al., 2006; Sadezky, 2005). SOA formation was also shown to be strongly reduced in the presence of water vapour (Sadezky, 2005). HCOOH, and to a lesser extent H_2O , are known to act as efficient scavengers for stabilized CI through the above-mentioned formation of hydroperoxy formates and hydroxy hydroperoxides. Consequently, the key reaction mechanisms leading to SOA and oligomer formation are in direct concurrence with the known reactions of the stabilized CI with HCOOH or H_2O to form low-molecular, volatile hydroperoxides. The observations point towards a direct implication of stabilized CI in the SOA and oligomer formation.

Therefore, we suggested in our previous study (Sadezky et al., 2006) that oligoperoxide formation is another, so far unknown gas-phase reaction of stabilized CI, which contributes to SOA formation. In our present work, we show that the observed formation of oligomers consisting of repeated CI-like chain units as main SOA constituents is not limited to enol ethers, but occurs in an analogous way for short-chain hydrocarbon alkenes.

To our knowledge, besides our previous study by Sadezky et al. (2006), formation of stable reaction products containing several linked CI-like units has not been reported previously for gas-phase ozonolysis. So far, such reactions have been observed for

14066

alkene-ozone reactions in the liquid phase only. Thus, recombination of two CI leading to the formation of cyclic geminal diperoxides (1,2,4,5-tetroxanes) was described as a minor reaction of stabilized CI during the ozonolysis of oleic acid (Zahardis and Petrucci, 2007; Reynolds et al., 2006; Zahardis et al., 2005). Oleic acid-ozone reactions in these studies take place in the condensed phase either in bulk solution with high reactant concentrations (Reynolds et al., 2006) or in liquid submicron aerosol droplets after diffusion of ozone into the particles (Zahardis and Petrucci, 2007; Zahardis et al., 2005). Moreover, 1,2,4,5-tetroxanes are known as common crystalline byproducts of many bulk liquid-phase ozonolysis reactions (Bunnelle, 1991). Formation of linear CI dimers in the liquid phase is mentioned by March (1992), these compounds are however reported to be unstable and to directly decompose into two carbonyl compounds and O₂. Tolocka et al. (2006) take into consideration a cyclic or linear dimer of two stabilized CI with an added H₂O, which then undergoes elimination of H₂O₂ either in the condensed particle phase or during the ionization process, for an unknown product observed in the mass spectra of SOA from gas-phase ozonolysis of α -pinene. The authors suggest that the linear dimer molecule, if formed, might be capped by the added H₂O.

Linear oligomerization of CI leading to stable long-chain oligoperoxides was so far only reported by Barton et al. (2005) and Barton et al. (2004) for liquid-phase ozonolysis of the hydrocarbon alkenes 2,3-dimethyl-2-butene ((CH₃)₂C=C(CH₃)₂), 3-methyl-2-pentene, and *trans*-2-hexene. As mentioned before, oligoperoxides identified as reaction products of the ozonolysis of 2,3-dimethyl-2-butene in the liquid phase by Barton et al. (2004) and in the gas phase in our present work show the same repetitive chain link of mass 74, which corresponds to the only Criegee Intermediate (CH₃)₂COO (*iso*-C₃-CI) formed by this alkene. Oligoperoxides identified by Barton et al. (2005) and Barton et al. (2004) are mainly cyclic hexamers or pentamers, with minor products consisting of linear chains endcapped by –OOH or –OH groups. Moreover, these oligomeric products were found by Barton et al. (2004) to be thermally stable when extracted and refluxed in methanol for a few hours, a behaviour that agrees with their

14067

observed stability in methanol used as solvent for the filter extraction in our work. Furthermore, Barton et al. (2004) observed a strong competition among the described formation of oligoperoxides consisting of CI-like units and well known liquid-phase reactions of the CI with compounds carrying hydroxylic functionalities to form small hydroperoxides (see above; Bunnelle, 1991). The authors reported oligoperoxide formation during liquid-phase ozonolysis of 2,3-dimethyl-2-butene to take place only in non-pronated solvents, such as pentane, while in methanol, the corresponding hydroperoxide, 2-methoxy-2-propyl hydroperoxide, was formed instead through reaction of the CI, (CH₃)₂COO (*iso*-C₃-CI), with MeOH. These observations of liquid-phase chemistry are in analogy to the suppression of SOA and oligomer formation during gas-phase enol ether ozonolysis in the presence of excess HCOOH or H₂O, as described in our previous work (Sadezky et al., 2006). The mechanistic analogies indicate that oligoperoxide formation takes place in similar ways in the liquid phase and in the gas phase, thus also confirming our suggestion by Sadezky et al. (2006) that the stabilized form of CI might be involved in the gas-phase reaction.

Addition of a CI to the double bond of the initial alkene, leading to formation of an 1,2-dioxolane, represents another reaction pathway of CI known from liquid-phase alkene ozonolysis (Bunnelle, 1991), in particular for vinyl ethers (Keul et al., 1985). A similar mechanism as a minor reaction pathway of stabilized CI has been attributed to products identified in the oleic acid/ozone and methyl oleate/ozone reaction systems (Mochida et al., 2006; Zahardis et al., 2006). Decomposition of the 1,2-dioxolane then leads to an aldehyde derived from the CI and a ketone representing the oxygenated initial alkene. For the small unsaturated ethers and alkenes studied in our work, these products are expected to be volatile, and consequently, this reaction pathway is not expected to contribute to SOA formation.

As mentioned in Sects. 3.2 and 3.3.1 of the present work, a comparison of the SOA mass and oligomer chain lengths obtained from ozonolysis of *trans*-3-hexene and EBE on the one hand, and 2,3-dimethyl-2-butene on the other hand, points towards a key role of stabilized CI in the SOA formation as well. The very low stabilization rate of the

14068

iso-C₃-CI ((CH₃)₂COO), which is less than 1% in the gas phase, correlates with much lower SOA mass and lower degrees of oligomerization from 2,3-dimethyl-2-butene in comparison with those from EBE and *trans*-3-hexene, which involve the isomer C₃-CI (C₂H₅CHOO) with stabilization rates between 20% and 40% (Kroll et al., 2002; Rickard et al., 1999).

However, the influence of excess cyclohexane added as OH radical scavenger on SOA mass described in Sect. 3.2 indicates also a contribution of radical chemistry to SOA formation, in addition to the chemistry of stabilized CI. The increase of SOA mass for the symmetric hydrocarbon alkenes *trans*-3-hexene and 2,3-dimethyl-2-butene in the presence of excess cyclohexane observed in our present work agrees with similar tendencies of formed SOA mass from β -pinene reported by Docherty and Ziemann (2003). Small vinyl ethers investigated in our previous work (Sadezky et al., 2006) and cyclohexene studied by Keywood et al. (2004), however, follow the opposite trend. Keywood et al. (2004) and Docherty and Ziemann (2003) explain the influence of cyclohexane as an OH radical scavenger by a decrease of the ratio [hydroperoxy radicals]/[organic peroxy radicals] in the reaction system, which, according to Keywood et al. (2004), especially affects the production pathways and chemistry of acyl radicals considered as key species in the formation of low-volatile compounds during cyclohexene and β -pinene ozonolysis. However, for the alkenes and enol ethers studied in our present and previous work (Sadezky et al., 2006), acyl radicals are not expected to contribute to the formation of high-molecular oligomers by any of their reaction pathways known so far, as discussed before in this section.

The detailed reaction mechanism of the observed oligomer formation in the gas phase, as well as the structures and precise identities of the starting and end groups "X" and "Y", remain so far an enigma and need further investigation. The observations of our present work allow us to identify the oligomer chain units and thus to confirm the systematic correlation between their chemical composition and that of the major CI formed during ozonolysis of the respective alkene. The entire oligomer structures, however, appear to be more complicated than those identified from liquid-phase ozonolysis

14069

by Barton et al. (2004) and Barton et al. (2005), which are either linear with -OOH or -OH as starting and end groups "X" and "Y", or cyclic without any fragments accounting for other than the repeated chain units. The numerous common features among the structures and chemical compositions of the oligomers originating from the different alkenes and enol ethers concerning not only the CI-like repeated chain units, but also the fragment ions and neutrals representing the starting and end groups X and Y (see Sect. 3.3.2), indicate a common mechanism of oligomer formation in the gas phase. The observations in the present work and in our previous study (Sadezky et al., 2006) cannot be explained by any classical reaction mechanisms established so far and must involve some new chemistry. The obvious key role of stabilized CI in SOA and oligomer formation, in combination with the observed influence of cyclohexane as OH radical scavenger on SOA yields, might, for example, point towards a mechanism based on so far unknown CI-radical reactions.

3.4 Copolymerization of chain units from different ozonolysis reactions

In order to investigate the role of the CI in relation to the role of the initial unsaturated compounds in the formation of oligomers, simultaneous gas-phase ozonolysis of *trans*-3-hexene and EVE was performed in the atmospheric simulation chamber. The MS spectrum of the SOA collected during this experiment is shown in Fig. 8.

Several of the most intense ion peaks are identified as oligomer ions consisting of CI-like chain units. These ion peaks are marked by red and green arrows in Fig. 8. Oligomer ions marked by red arrows are of *m/z* similar to those of oligomer (a) ions formed during ozonolysis of *trans*-3-hexene solely (Fig. 2b and Table 2). According to our results presented in the Sect. 3.3, these ions might therefore comprise only chain units of mass 74 (C₃H₆O₂), with *n*=1 and *n*=2 for the two most intense ions 305 and 379 in Fig. 8. Oligomer ions marked by green arrows are deduced from ions marked by red arrows by addition of multiples of $\Delta m/z$ 46. Thus, these ions eventually contain combinations of both chain units 74 (C₃H₆O₂) and 46 (CH₂O₂). The most intense ions of this type are of *m/z* 351 (*m/z* 351=*m/z* 305 + $\Delta m/z$ 46), *m/z* 397 (*m/z* 397=*m/z*

14070

305 + 2×Δ m/z 46), and m/z 425 (m/z 425= m/z 379 + Δ m/z 46) (Fig. 8).

Some ions between m/z 150 and 300 are identified from MS/MS experiments as fragment ions of higher parent ions and are listed separately in Fig. 8.

MS/MS spectra of the pseudomolecular ions 305 (marked by a red arrow in Fig. 8) and 351 (marked by a green arrow in Fig. 8) are exemplarily given in Figs. 9a and b, and the observed main fragmentation pathways of these two parent ions are schematically displayed in Figs. 10a and b.

The MS/MS spectrum of the parent ion 305 (Figs. 9a and 10a) confirms that its structure is indeed similar to those of the type (a) oligomer ions formed during gas-phase ozonolysis of *trans*-3-hexene solely, which are described in Sect. 3.3 of this work. Its fragmentation pathways are identical to those of its higher homologue 379 observed from ozonolysis of *trans*-3-hexene solely (Figs. 4a and 6a), and show the presence of one chain unit 74 ($C_3H_6O_2$), as expected (Fig. 2b and Table 2).

The MS/MS spectrum of the parent ion 351 (Figs. 9b and 10b) reproduces the fragmentation pathways observed for the parent ion 305 (Figs. 9a and 10a), but includes an additional loss of a neutral of mass 46. This result shows that the parent ion 351, and more generally all pseudomolecular ions marked by green arrows in Fig. 8, correspond to ions initially formed from ozonolysis of *trans*-3-hexene (marked by red arrows in Fig. 8) that contain additional chain units of mass 46.

The formation of such ions signifies that copolymerization of the two CI-like chain units 74 ($C_3H_6O_2$, C_3 -CI from *trans*-3-hexene) and 46 (CH_2O_2 , C_1 -CI from EVE) takes place. The two chain units arise from CI that are simultaneously present in the reaction system, but are formed independently during gas-phase ozonolysis of *trans*-3-hexene and EVE. The observed copolymerization of the two chain units under these experimental conditions indicates that oligomer formation might be based on reactions of the free CI itself after complete dissociation of the primary ozonide.

Copolymerization of CI-like chain units formed from different alkenes was also observed by Barton et al. (2005) for the simultaneous ozonolysis of 2,3-dimethyl-2-butene and 3-methyl-2-pentene in the liquid phase. The authors identified a variety

14071

of oligomeric molecules, which follow similar structural principles as those obtained by separate ozonolysis of each alkene (see Sect. 3.3.3), but contain a mixture of the chain units formed by both unsaturated compounds, that is, acetone carbonyl oxide (*iso*- C_3 -CI, $(CH_3)_2COO$) from 2,3-dimethyl-2-butene, and butanone carbonyl oxide (C_4 -CI, C_3H_7CHOO) and acetaldehyde from 3-methyl-2-pentene.

4 Conclusions

In the present work, we investigate secondary organic aerosol (SOA) formation during gas phase ozonolysis of an enol ether, ethyl butenyl ether (EBE), and three symmetric alkenes, *trans*-3-hexene, *trans*-4-octene, and 2,3-dimethyl-2-butene. Chemical analysis of the formed SOA is performed employing the ESI(+)/MS-TOF, the ESI(+)/MS/MS-TOF, and the accurate ESI(+)-FTICR MS/MS technique. These techniques allow to identify and thoroughly characterize oligomeric products in the mass range 200 to 800 u as main constituents of the SOA for all alkenes and the enol ether studied.

Similar oligomers in SOA formed by gas phase ozonolysis of small unsaturated compounds have been identified for the first time for a series of small alkyl vinyl ethers (AVE) and ethyl propenyl ether (EPE) in our previous study (Sadezky et al., 2006). The results of our present work corroborate our findings of Sadezky et al. (2006), in particular the essential role of Criegee Intermediates (CI), initially formed in the gas-phase, in oligomer and SOA formation: oligomer chain units are shown to systematically have the same chemical composition as the respective main Criegee Intermediate (CI) formed by the gas-phase ozonolysis reaction. Fragmentation spectra (MS/MS) of oligomer pseudomolecular ions furthermore reveal strong structural analogies among oligomers formed from ozonolysis of different alkenes and enol ethers, thus indicating a common structural principle and formation mechanism.

We suggested in our previous study (Sadezky et al., 2006) that CI in their stabilized form undergo oligomerization in the gas-phase according to a new, so far unknown reaction mechanism that leads to the formation of oligoperoxidic chains. In our present

14072

work, we show that our observations by Sadezky et al. (2006) are not limited to enol ethers, but analogously apply to a variety of short-chain hydrocarbon alkenes. Therefore, we propose oligoperoxide formation as a new, general reaction pathway of stabilized CI in the gas phase, eventually with participation of CI-radical reactions. The detailed reaction mechanism, however, is so far unknown and needs further investigation.

Moreover, we report an example for copolymerization of different CI independently produced during simultaneous gas-phase ozonolysis of two different unsaturated compounds, leading to the formation of oligomers with mixed CI-like chain units. These observations further point towards a direct participation of free CI in the oligomerization mechanism, which is independent of their formation process from the original unsaturated compound.

The smallest unsaturated organic compound shown to produce SOA during its gas-phase ozonolysis under atmospheric conditions is methyl vinyl ether (MVE) with three carbon atoms (Klotz et al., 2004). Before, it was widely accepted in the literature, that seven or more C atoms are required from non-cyclic unsaturated hydrocarbons, six for cyclic unsaturated species to initiate SOA formation from ozonolysis (Seinfeld and Pankow, 2003). The classical reaction pathways of gas-phase ozonolysis established for such large compounds, which lead to low-volatile products identified as SOA constituents, however, cannot explain SOA formation from small and structurally simple unsaturated reactants, such as MVE.

While Klotz et al. (2004) could not give any clues about the chemical composition and formation mechanism of the SOA formed from ozonolysis of methyl vinyl ether (MVE), the oligomeric compounds newly discovered and characterized in our previous work (Sadezky et al., 2006) as reaction products of gas-phase ozonolysis of several similar enol ethers containing five to seven carbon atoms, provided a sound explanation. By the identification of analogous oligomeric SOA constituents for the compounds studied in our present work, we show that formation of such oligomers occurs for a wider range of small oxygenated as well as hydrocarbon alkenes, and might thus be a general, new

14073

reaction pathway that mainly depends on the nature of the Criegee Intermediate (CI).

The high-molecular oligoperoxides formed in the gas phase by the new mechanism, which we suggested to involve the stabilized form of CI (Sadezky et al., 2006), might then initiate nucleation, and thus lead to the observed formation of new SOA particles. It thus represents a new way to SOA formation especially from gas-phase ozonolysis of unsaturated compounds with few carbon atoms and simple structures.

According to Klotz et al. (2004), new SOA particle formation from methyl vinyl ether (MVE) occurs only during its gas-phase ozonolysis, but not by its reactions with OH or NO₃ radicals, the two other major pathways of atmospheric degradation. This observation further supports the key role of the CI in SOA formation as an intermediate species specific to ozonolysis. In the troposphere, stabilized CI are expected to mainly react with water vapour, a reaction that has been shown to be in direct concurrence with oligomer and new SOA particle formation during the ozonolysis of enol ethers (Sadezky et al., 2006; Sadezky, 2005). The relevance of the described oligoperoxide formation for SOA formation in the atmosphere has therefore to be further investigated.

Acknowledgements. The study was financially supported by the European Science Foundation (ESF) through a grant for a researcher's visit within the INTROP exchange program.

References

- Altieri, K. E., Carlton, A. G., Lim, H.-J., Turpin, B. J., and Seitzinger, S. P.: Evidence for oligomer formation in clouds: Reactions of isoprene oxidation products, *Environ. Sci. Technol.*, 40, 4956–4960, 2006.
- Barton, M., Ebdon, J. R., Foster, A. B., and Rimmer, S.: Ozonolysis of tetramethylethylene: Characterization of cyclic and open-chain oligoperoxidic products, *J. Org. Chem.*, 69, 6967–6973, 2004.
- Barton, M., Ebdon, J. R., Foster, A. B., and Rimmer, S.: Complete ozonolysis of alkyl substituted ethenes at –60°C: Distributions of ozonide and oligomeric products, *Org. Biomol. Chem.*, 3, 1323–1329, 2005.

14074

- Bunnelle, W. H.: Preparation, properties, and reactions of carbonyl oxides, *Chem. Rev.*, 91, 335–362, 1991.
- Calvert J. G., Atkinson R., Kerr J. A., Madronich S., Moortgat G. K., Wallington T. J., and Yarwood G.: The mechanisms of atmospheric oxidation of the alkenes, Oxford University Press, 2000.
- 5 Docherty, K. S. and Ziemann, P. J.: Effects of stabilized Criegee Intermediate and OH radical scavengers on aerosol formation from reactions of β -pinene with O_3 , *Aerosol Sci. Technol.*, 37, 877–891, 2003.
- Docherty, K. S., Wu, W., Lim, Y. B., and Ziemann, P. J.: Contributions of organic peroxides to secondary aerosol formed from reactions of monoterpenes with O_3 , *Environ. Sci. Technol.*, 10 39, 4049–4059, 2005.
- Dreyfus, M. A., Tolocka, M. P., Dodds, S. M., Dykins, J., and Johnston, M. V.: Cholesterol ozonolysis: Kinetics, mechanism and oligomer products, *J. Phys. Chem. A*, 109, 6242–6248, 2005.
- 15 Finlayson, B. J., Pitts, J. N., and Akimoto, H.: Production of vibrationally excited OH in chemiluminescent ozone-olefin reactions, *Chem. Phys. Lett.*, 12, 495–498, 1972.
- Fuzzi, S., Andreae, M. O., Huebert, B. J., Kulmala, M., Bond, T. C., Boy, M., Doherty, S. J., Guenther, A., Kanakidou, M., Kawamura, K., Kerminen, V.-M., Lohmann, U., Russell, L. M., and Pöschl, U.: Critical assessment of the current state of scientific knowledge, terminology, 20 and research needs concerning the role of organic aerosols in the atmosphere, climate, and global change, *Atmos. Chem. Phys.*, 6, 2017–2038, 2006,
<http://www.atmos-chem-phys.net/6/2017/2006/>.
- Gao, S., Nga, L. N., Keywood, M., Varutbangkul, V., Bahreini, R., Nenes, A., He, J., Yoo, K. Y., Beauchamp, J. L., Hodyss, R. P., Flagan, R. C., and Seinfeld, J. H.: Particle phase acidity 25 and oligomer formation in secondary organic aerosol, *Environ. Sci. Technol.*, 38, 6582–6589, 2004.
- Gross, D. S., Gälli, M. E., Kalberer, M., Prevot, A. S. H., Dommen, J., Alfarra, M. R., Duplissy, J., Gaeggeler, K., Gascho, A., Metzger, A., and Baltensperger, U.: Real-time measurement of oligomeric species in secondary organic aerosol with the aerosol time-of-flight mass spectrometer, *Anal. Chem.*, 78, 2130–2137, 2006.
- 30 Guzman, M. I., Colussi, A. J., and Hoffmann, M. R.: Photoinduced oligomerization of aqueous pyruvic acid, *J. Phys. Chem. A*, 110, 3619–3626, 2006.
- Hamilton, J. F., Lewis, A. C., Reynolds, J. C., Carpenter, L. J., and Lubben, A.: Investigating the

14075

- composition of organic aerosol resulting from cyclohexene ozonolysis: Low molecular weight and heterogeneous reactions products, *Atmos. Chem. Phys.*, 6, 4973–4984, 2006,
<http://www.atmos-chem-phys.net/6/4973/2006/>.
- Horie, O., Neeb, P., and Moortgat, G. K.: The reactions of the criegee-intermediate CH_3CHO 5 in the gas-phase ozonolysis of 2-butene isomers, *Int. J. Chem. Kin.*, 29, 461–468, 1997.
- Kalberer, M., Paulsen, D., Sax, M., Steinbacher, M., Dommen, J., Prevot, A. S. H., Fisseha, R., Weingartner, E., Frankevich, V., Zenobi, R., and Baltensperger, U.: Identification of polymers as major components of atmospheric organic aerosols, *Science*, 303, 1659–1662, 2004.
- Kanakidou, M., Seinfeld, J. H., Pandis, S. N., Barnes, I., Dentener, F. J., Facchini, M. C., van Dingenen, R., Ervens, B., Nenes, A., Nielsen, C. J., Swietlicki, E., Putaud, J. P., Balkanski, 10 Y., Fuzzi, S., Hjorth, J., Moortgat, G. K., Winterhalter, R., Myhre, C. E. L., Tsigaridis, K., Vignati, E., Stephanou, E. G., and Wilson, J.: Organic aerosol and global climate modelling: A review, *Atmos. Chem. Phys.*, 5, 1053–1123, 2005,
<http://www.atmos-chem-phys.net/5/1053/2005/>.
- 15 Keul, H., Choi, H. S., and Kuczkowski, R. L.: Ozonolysis of enol ethers. Formation of 3-alkoxy-1,2-dioxolanes by concerted addition of a carbonyl oxide to an enol ether, *J. Org. Chem.*, 50, 3365–3371, 1985.
- Keywood, M. D., Kroll, J. H., Varutbangkul, V., Bahreini, R., Flagan, R. C., and Seinfeld, J. H.: Secondary organic aerosol formation from cyclohexene ozonolysis: Effect of OH scavenger 20 and the role of radical chemistry, *Environ. Sci. Technol.*, 38, 3343–3350, 2004.
- Klotz, B., Barnes, I., and Imamura, T.: Product study of the gas-phase reactions of O_3 , OH and NO_3 radicals with methyl vinyl ether, *Phys. Chem. Chem. Phys.*, 6, 1725–1734, 2004.
- Koch, S., Winterhalter, R., Uhrek, E., Kolloff, A., Neeb, P., and Moortgat, G. K.: Formation of new particles in the gas-phase ozonolysis of monoterpenes, *Atmos. Environ.*, 34, 4031– 25 4042, 2000.
- Kroll, J. H., Donahue, N. M., Cee, V. J., Demerjian, K. L., and Anderson, J. G.: Gas-phase ozonolysis of alkenes: Formation of OH from anti carbonyl oxides, *J. Am. Chem. Soc.*, 124, 8518–8519, 2002.
- Lockley, J. E., Ebdon, J. R., Rimmer, S., and Tabner, B. J.: Polymerization of methyl methacrylate initiated by ozonates of tetramethylethene, *Polymer*, 42, 1797–1807, 2001.
- March, J.: *Advanced organic chemistry: reactions, mechanisms, and structure* (fourth edition), John Wiley & Sons, Inc., 1992.
- Mochida, M., Katrib, Y., Jayne, J. T., Worsnop, D. R., and Martin, S. T.: The relative importance

14076

- of competing pathways for the formation of high-molecular-weight peroxides in the ozonolysis of organic aerosol particles, *Atmos. Chem. Phys.*, 6, 4851–4866, 2006, <http://www.atmos-chem-phys.net/6/4851/2006/>.
- 5 Murphy, S. M., Sorooshian, A., Kroll, J. H., Ng, N. L., Chabra, P., Tong, C., Surratt, J. D., Knipping, E., Flagan, R. C., and Seinfeld, J. H.: Secondary aerosol formation from atmospheric reactions of aliphatic amines, *Atmos. Chem. Phys.*, 7, 2313–2337, 2007, <http://www.atmos-chem-phys.net/7/2313/2007/>.
- Neeb, P., Horie, O., and Moortgat, G. K.: Formation of secondary ozonides in the gas-phase ozonolysis of simple alkenes, *Tetrahedron Lett.*, 37, 9297–9300, 1996.
- 10 Neeb, P., Sauer, F., Horie, O., and Moortgat, G. K.: Formation of hydroxymethyl hydroperoxide and formic acid in alkene ozonolysis in the presence of water vapour, *Atmos. Environ.*, 31, 1417–1423, 1997.
- Neeb, P., Horie, O., and Moortgat, G. K.: The ethene-ozone reaction in the gas phase, *J. Phys. Chem. A*, 102, 6778–6785, 1998.
- 15 Pöschl, U.: Atmospheric aerosols: Composition, transformation, climate and health effects, *Angew. Chem. Int. Ed.*, 44, 7520–7540, 2005.
- Reynolds, J. C., Last, D. J., McGillen, M., Nijs, A., Horn, A. B., Percival, C., Carpenter, L. J., and Lewis, A. C.: Structural analysis of oligomeric molecules formed from the reaction products of oleic acid ozonolysis, *Environ. Sci. Technol.*, 40, 6674–6681, 2006.
- 20 Rickard, A. R., Johnson, D., McGill, C. D., and Marston, G.: OH yields in the gas-phase reactions of ozone with alkenes, *J. Phys. Chem. A*, 103, 7656–7664, 1999.
- Römpf, A., Taban, I. M., Mihalca, R., Duursma, M. C., Mize, T. H., McDonnell, L. A., and Heeren, R. M. A.: Examples of Fourier transform ion cyclotron resonance mass spectrometry developments: from ion physics to remote access biochemical mass spectrometry, *Eur. J. Mass. Spectrom.*, 11, 443–456, 2005.
- 25 Sadezky A.: Ozonolyse d'éthers insaturés: Etudes des mécanismes en phase gazeuse et de la formation d'aérosol organique secondaire, PhD Thesis, University of Orleans, 2005.
- Sadezky, A., Chaimbault, P., Mellouki, A., Römpf, A., Winterhalter, R., Moortgat, G. K., and Le Bras, G.: Formation of secondary organic aerosol and oligomers from the ozonolysis of enol ethers, *Atmos. Chem. Phys.*, 6, 5009–5024, 2006, <http://www.atmos-chem-phys.net/6/5009/2006/>.
- 30 Seinfeld, J. H. and Pankow, J. F.: Organic atmospheric particular material, *Annu. Rev. Phys. Chem.*, 54, 121–140, 2003.

14077

- Surratt, J. D., Murphy, S. M., Kroll, J. H., Nga, L. N., Hildebrandt, L., Sorooshian, A., Szmigielski, R., Vermeylen, R., Maenhaut, W., Claeys, M., Flagan, R. C., and Seinfeld, J. H.: Chemical composition of secondary organic aerosol formed from the photooxidation of isoprene, *J. Phys. Chem. A*, 110, 9665–9690, 2006.
- 5 Tobias, H. J., Docherty, K. S., Beving, D. E., and Ziemann, P. J.: Effect of relative humidity on the chemical composition of secondary organic aerosol formed from reactions of 1-tetradecene and O₃, *Environ. Sci. Technol.*, 34, 2116–2125, 2000.
- Tobias, H. J. and Ziemann, P. J.: Thermal desorption mass spectrometric analysis of organic aerosol from reactions of 1-tetradecene and O₃ in the presence of alcohols and carboxylic acids, *Environ. Sci. Technol.*, 34, 2105–2115, 2000.
- 10 Tolocka, M. P., Jang, M., Ginter, J. M., Cox, F. J., Kamens, R. M., and Johnston, M. V.: Formation of oligomers in secondary organic aerosol, *Environ. Sci. Technol.*, 38, 1428–1434, 2004.
- Tolocka, M. P., Heaton, K. J., Dreyfus, M. A., Wang, S., Zordan, C. A., Saul, T. D., and Johnston, M. V.: Chemistry of particle inception and growth during α -pinene ozonolysis, *Environ. Sci. Technol.*, 40, 1843–1848, 2006.
- 15 Zahardis, J., LaFranchi, B. W., and Petrucci, G. A.: Photoelectron resonance capture ionization-aerosol mass spectrometry of the ozonolysis products of oleic acid particles: Direct measure of higher molecular weight oxygenates, *J. Geophys. Res.*, 110, D08307, doi:10.1029/2004JD005336, 2005.
- Zahardis, J., LaFranchi, B. W., and Petrucci, G. A.: Direct observation of polymerization in the oleic acid-ozone heterogeneous reaction system by photoelectron resonance capture ionization aerosol mass spectrometry, *Atmos. Environ.*, 40, 1661–1670, 2006.
- Zahardis, J. and Petrucci, G. A.: The oleic acid-ozone heterogeneous reaction system: Products, kinetics, secondary chemistry, and atmospheric implications of a model system - a review, *Atmos. Chem. Phys.*, 7, 1237–1274, 2007, <http://www.atmos-chem-phys.net/7/1237/2007/>.
- 25 Ziemann, P. J.: Evidence for low-volatility diacyl peroxides as a nucleating agent and major component of aerosol formed from reactions of O₃ with cyclohexene and homologous compounds, *J. Phys. Chem. A*, 106, 4390–4402, 2002.
- 30 Ziemann, P. J.: Formation of alkoxyhydroperoxy aldehydes and cyclic peroxyhemiacetals from reactions of cyclic alkenes with O₃ in the presence of alcohols, *J. Phys. Chem. A*, 107, 2048–2060, 2003.

14078

Table 1. Total SOA masses M_0 ($\mu\text{g}/\text{m}^3$) formed, initial mixing ratios of reactants and cyclohexane (C_6H_{12}), and types of major CI formed in the gas-phase ozonolysis reactions of the unsaturated compounds studied in this work.

Alkene	[alkene] ₀ [ppm]	[ozone] ₀ [ppm]	[C ₆ H ₁₂] ₀ [ppm]	Type of CI	M (SOA) [$\mu\text{g}/\text{m}^3$]
EBE ($\text{C}_2\text{H}_5\text{O}-\text{CH}=\text{CHC}_2\text{H}_5$)	15	8	–	C ₃ -CI	250
<i>trans</i> -3-hexene ($\text{C}_2\text{H}_5\text{CH}=\text{CHC}_2\text{H}_5$)	15	8	–	C ₃ -CI	160
“	15	8	300	C ₃ -CI	400
<i>trans</i> -4-octene ($\text{C}_3\text{H}_7\text{CH}=\text{CHC}_3\text{H}_7$)	15	8	–	C ₄ -CI	300
2,3-dimethyl-2-butene ($(\text{CH}_3)_2\text{C}=\text{C}(\text{CH}_3)_2$)	15	8	300	<i>iso</i> -C ₃ -CI	40
“	15	8	–	<i>iso</i> -C ₃ -CI	3
EVE ($\text{C}_2\text{H}_5\text{O}-\text{CH}=\text{CH}_2$)	6	8	–	C ₁ -CI	**
+	+			+	
<i>trans</i> -3-hexene ($\text{C}_2\text{H}_5\text{CH}=\text{CHC}_2\text{H}_5$)	8			C ₃ -CI	

** not measured

14079

Table 2. Oligomer pseudomolecular ion series detected by ESI(+)/MS-TOF in the SOA formed during ozonolysis of enol ethers and alkenes (n: minimum number of chain carrier units determined by MS/MS experiments) (MW: molar weight [g/mol]).

Ether	Ion Series (m/z)										
	n	n=0	n=1	n=2	n=3	n=4	n=5	n=6	n=7	n=8	n=9
Ethyl propenyl ether (MW 86 g/mol)			339	399	459	519	579	639	699	759	(a)
EPE, $\text{C}_3\text{H}_5\text{OCH}=\text{CHCH}_3$ (Sadezky et al., 2006)		265	325	385	445						(C)
		293	353	413	473	533					(D)
					489	549	609	669	729	789	(E)
Ethyl vinyl ether (MW 72 g/mol)			283	329	375	421	467	513			(a)
EVE, $\text{C}_3\text{H}_5\text{OCH}=\text{CH}_2$ (Sadezky et al., 2006)				345	391	437	483				(b)
Ethyl butenyl ether (MW 100 g/mol)			321	395	469	543	617	691			(a)
EBE, $\text{C}_2\text{H}_5\text{OCH}=\text{CHC}_2\text{H}_5$ (this work)			279	353	427	501		647	721	795	(B)
					437	511	585				(F)
			305	379	453	527	601				•↓
<i>trans</i>-3-hexene (MW 84 g/mol)			305	379	453	527					(a)
$\text{C}_2\text{H}_5\text{CH}=\text{CHC}_2\text{H}_5$ (this work)			321	395	469						(b)
2,3-dimethyl-2-butene (MW 84 g/mol)		231	305	379	453						(a)
$(\text{CH}_3)_2\text{C}=\text{C}(\text{CH}_3)_2$ (this work)		245	321	395							(b)
			263	337	411	495	559				(B)
<i>trans</i>-4-octene (MW 112 g/mol)		273	361	449	537						(a)
$\text{C}_3\text{H}_7\text{CH}=\text{CHC}_3\text{H}_7$ (this work)		289	377	465	553						(b)
			347	435							(C)
			391	479							(E)
				417	505	593					(F)
				401	489						(G)

14080

Table 3a. ESI(+)/MS/MS-FTICR measurements:
Calculated elemental compositions of parent ions, fragment ions and fragmented neutral molecules for the red-marked fragmentation pathway of the pseudomolecular oligomer ion 379 formed from *trans*-3- hexene (see Fig. 6a).

Accurate mass (u)	Elemental composition	Exact mass (u)	Absolute mass error (mDa)	Relative mass error (ppm)
379.19565	C₁₇H₃₁O₉	379.1962	-0.6094	-1.6071
parent ion	C ₁₆ H ₂₇ O ₁₀	379.1598	35.776	94.3472
[X-[74] ₂ -Y + H] ⁺	C ₁₈ H ₃₅ O ₈	379.2326	-36.9949	-97.5614
	C ₁₅ H ₂₃ O ₁₁	379.1234	72.1616	190.3015
	C ₁₉ H ₃₉ O ₇	379.269	-73.3804	-193.5158
146.13120	C₈H₁₆O₂	146.1306	0.52	3.5584
initially fragmented neutral	C ₁₁ H ₁₄	146.1095	21.6494	148.1507
X or Y	C ₇ H ₁₄ O ₃	146.0942	36.9055	252.5505
	C ₆ H ₁₀ O ₄	146.0579	73.291	501.5427
233.06445	C₉H₁₃O₇	233.0655	-1.1294	-4.8459
fragment ion	C ₈ H ₉ O ₈	233.0291	35.256	151.2715
[Y-[74] ₂ + H] ⁺	C ₁₀ H ₁₇ O ₆	233.1019	-37.5149	-160.9634
or [X-[74] ₂ + H] ⁺				
74.03673	C₃H₆O₂	74.0367	0.0495	0.6688
neutral	C ₂ H ₂ O ₃	74.0003	36.336	490.7834
chain carrier 74	C ₄ H ₁₀ O	74.0731	-36.435	-492.1211
159.02772	C₆H₇O₅	159.0287	-1.0799	-6.7906
fragment ion	C ₅ H ₃ O ₆	158.9924	35.3056	222.0084
[Y-[74] + H] ⁺	C ₇ H ₁₁ O ₄	159.0651	-37.4654	-235.5896
or [X-[74] + H] ⁺	C ₈ H ₁₅ O ₃	159.1015	-73.8509	-464.3887
74.0332*	C₃H₆O₂	74.0367	0.5204*	7.029*
neutral	C ₄ H ₁₀ O	74.0731	-35.865	484.4185
chain carrier 74	C ₂ H ₂ O ₃	74.0003	36.906	498.4784
84.9936*	C₃HO₃	84.992	1.5796*	18.585*
fragment ion	C ₄ H ₅ O ₂	85.0284	-34.8058	-409.5093
[Y + H] ⁺ or [X + H] ⁺	C ₅ H ₉ O	85.0647	-71.1914	-837.6037

* Accurate mass values from ESI(+)/MS/MS-TOF measurements (Fig. 4a) due to the strong decrease of sensitivity of the FTICR analyzer for ions with *m/z* below 100 u.

14081

Table 3b. ESI(+)/MS/MS-FTICR measurements:
Calculated elemental compositions of parent ions, fragment ions and fragmented neutral molecules for the violet-marked fragmentation pathway of the pseudomolecular oligomer ion 395 formed from EBE (see Fig. 5c).

Accurate mass (u)	Elemental composition	Exact mass (u)	Absolute mass error (mDa)	Relative mass error (ppm)
395.19255	C₁₇H₃₁O₁₀	395.1911	1.3759	3.4816
parent ion	C ₁₈ H ₃₅ O ₉	395.2275	-35.0095	-88.5885
[X-[74] ₂ -Y + H] ⁺	C ₁₆ H ₂₇ O ₁₁	395.1547	37.7614	95.5519
	C ₁₉ H ₃₉ O ₈	395.2639	-71.3951	-180.6587
(120.08194) [#]	C₅H₁₂O₃	120.0786	(3.2956)[#]	(27.445)[#]
initially fragmented neutral	C ₉ H ₁₂	120.0939	(-11.9604) [#]	(-99.6026) [#]
X or Y	C ₈ H ₈ O	120.0575	(24.425) [#]	(203.4031) [#]
	C ₄ H ₈ O ₄	120.0422	(39.6811) [#]	(330.4503) [#]
275.11061	C₁₂H₁₉O₇	275.1125	-1.9196	-6.9777
fragment ion	C ₁₁ H ₁₅ O ₈	275.0761	34.4658	125.2797
[Y-[74] ₂ + H] ⁺	C ₁₃ H ₂₃ O ₆	275.1489	-38.3051	-139.2352
or [X-[74] ₂ + H] ⁺				
74.03611	C₃H₆O₂	74.0367	-0.6695	-9.0431
neutral	C ₂ H ₂ O ₃	74.0003	35.7159	482.4132
chain carrier 74	C ₄ H ₁₀ O	74.0731	-37.055	-500.4995
201.07450	C₉H₁₃O₅	201.0757	-1.2501	-6.2172
fragment ion	C ₈ H ₉ O ₆	201.0393	35.1353	174.7376
[Y-[74] + H] ⁺	C ₁₀ H ₁₇ O ₄	201.1121	-37.6356	-187.1722
or [X-[74] + H] ⁺				

[#] Higher mass error than expected due to instrumental problems.

14082

Table 3c. ESI(+)/MS/MS-FTICR measurements:

Calculated elemental compositions of parent ions, fragment ions and fragmented neutral molecules for the violet-marked fragmentation pathway of the pseudomolecular oligomer ion 379 formed from 2,3-dimethyl-2-butene (see Fig. 6b).

Accurate mass (u)	Elemental composition	Exact mass (u)	Absolute mass error (mDa)	Relative mass error (ppm)
379.19574	C₁₇H₃₁O₉	379.1962	-0.5194	-1.3697
parent ion	C ₁₆ H ₂₇ O ₁₀	379.1598	35.866	94.5845
[X-[74] ₂ -Y + H] ⁺	C ₁₈ H ₃₅ O ₈	379.2326	-36.9049	-97.3241
	C ₁₅ H ₂₃ O ₁₁	379.1234	72.2516	190.5388
	C ₁₉ H ₃₉ O ₇	379.269	-73.2904	-193.2784
120.07937	C₅H₁₂O₃	120.0786	0.7255	6.0426
initially fragmented neutral	C ₉ H ₁₂	120.0939	-14.5304	-121.0072
X or Y	C ₈ H ₈ O	120.0575	21.855	182.0049
	C ₄ H ₈ O ₄	120.0422	37.1111	309.0549
259.11637	C₁₂H₁₉O₆	259.1176	-1.245	-4.8048
fragment ion	C ₁₁ H ₁₅ O ₇	259.0812	35.1405	135.6163
[Y-[74] ₂ + H] ⁺	C ₁₃ H ₂₃ O ₅	259.154	-37.6305	-145.2261
or [X-[74] ₂ + H] ⁺				
74.03671	C₃H₆O₂	74.0367	-0.0695	-0.9389
neutral	C ₂ H ₂ O ₃	74.0003	36.3159	490.5134
chain carrier 74	C ₄ H ₁₀ O	74.0731	-36.455	-492.3914
185.07966	C₉H₁₃O₄	185.0808	-1.1755	-6.3513
fragment ion	C ₈ H ₉ O ₅	185.0444	35.21	190.2419
[Y-[74] + H] ⁺	C ₁₀ H ₁₇ O ₃	185.1172	-37.561	-202.9445
or [X-[74] + H] ⁺				

14083

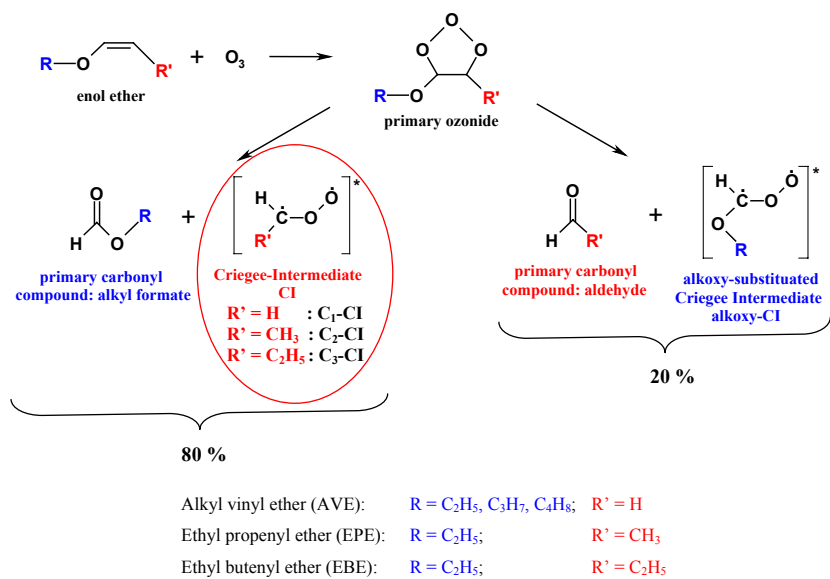
Table 3d. ESI(+)/MS/MS-FTICR measurements:

Calculated elemental compositions of parent ions, fragment ions and fragmented neutral molecules for the violet-marked fragmentation pathway of the pseudomolecular oligomer ion 449 formed from *trans*-4-octene (see Fig. 6c).

Accurate mass (u)	Elemental composition	Exact mass (u)	Absolute mass error (mDa)	Relative mass error (ppm)
449.27489	C₂₂H₄₁O₉	449.2745	0.3801	0.8462
parent ion	C ₂₃ H ₄₅ O ₈	449.3108	-36.0053	-80.1409
[X-[88] ₂ -Y + H] ⁺	C ₂₁ H ₃₇ O ₁₀	449.2381	36.7656	81.8333
	C ₂₄ H ₄₉ O ₇	449.3472	-72.3908	-161.128
	C ₂₀ H ₃₃ O ₁₁	449.2017	73.1512	162.8204
(148.11188) [#]	C₇H₁₆O₃	(148.1099)[#]	(1.9354)[#]	(13.0674)[#]
initially fragmented neutral	C ₁₁ H ₁₆	(148.1252) [#]	(-13.3206) [#]	(-89.9363) [#]
X or Y	C ₁₀ H ₁₂ O	(148.0888) [#]	(23.0648) [#]	(155.726) [#]
	C ₆ H ₁₂ O ₄	(148.0735) [#]	(38.3209) [#]	(258.7298) [#]
	C ₅ H ₈ O ₅	(148.0371) [#]	(74.7064) [#]	(504.3922) [#]
301.16301	C₁₅H₂₅O₆	301.1645	-1.5552	-5.1641
fragment ion	C ₁₄ H ₂₁ O ₇	301.1281	34.8302	115.6523
[Y-[88] ₂ + H] ⁺	C ₁₆ H ₂₉ O ₅	301.2009	-37.9407	-125.9806
or [X-[88] ₂ + H] ⁺	C ₁₀ H ₂₁ O ₁₀	301.1129	50.0863	166.3094
88.05210	C₄H₈O₂	88.0524	-0.3296	-3.7432
neutral	C ₃ H ₄ O ₃	88.016	36.0559	409.4839
chain carrier 88	C ₅ H ₁₂ O	88.0888	-36.7151	-416.9704
	C ₂ O ₄	87.9796	72.4414	822.711
213.11091	C₁₁H₁₇O₄	213.1121	-1.2256	-5.7512
fragment ion	C ₁₀ H ₁₃ O ₅	213.0757	35.1598	164.9834
[Y-[88] + H] ⁺	C ₁₂ H ₂₁ O ₃	213.1485	-37.6111	-176.4859
or [X-[88] + H] ⁺				

[#] Higher mass error than expected due to instrumental problems.

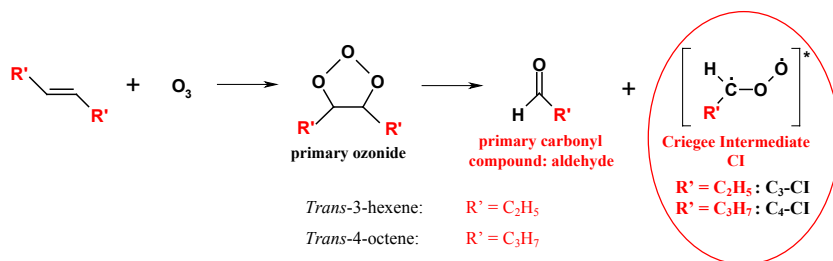
14084



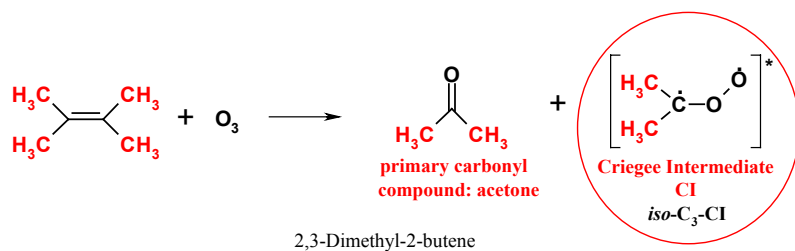
(a)

Fig. 1. General mechanism of the gas-phase ozonolysis of enol ethers and symmetric alkenes
(a) Enol ethers.

14085



(b)



(c)

Fig. 1. (b) *Trans*-3-hexene and *trans*-4-octene. (c) 2,3-Dimethyl-2-butene.

14086

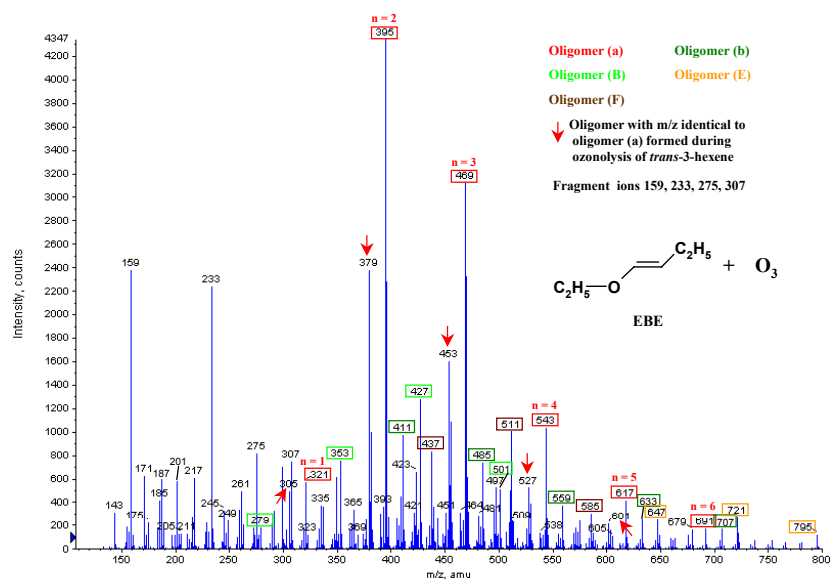


Fig. 2a. ESI(+)/MS-TOF mass spectrum of SOA formed during the gas phase ozonolysis of EBE (initial mixing ratios: 8 ppm ozone, 15 ppm EBE).

14087

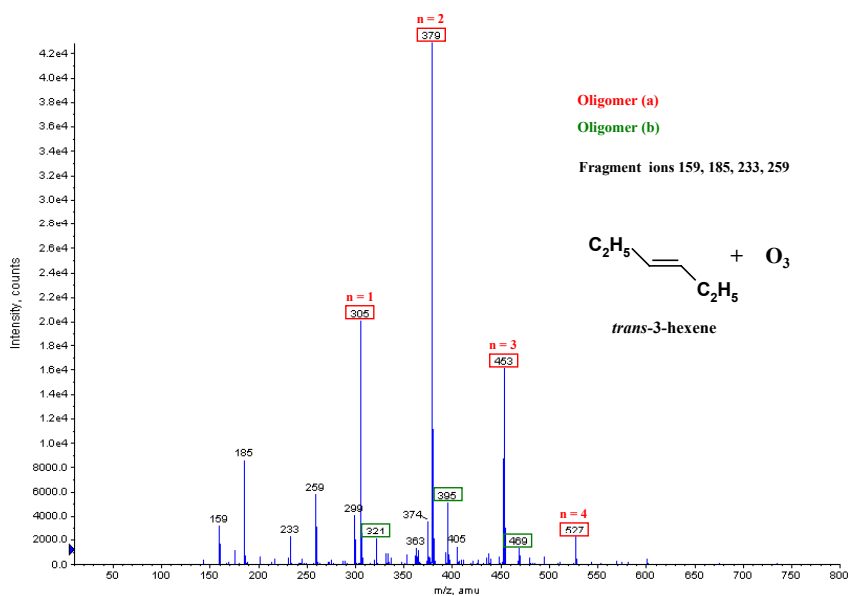


Fig. 2b. ESI(+)/MS-TOF mass spectrum of SOA formed during the gas phase ozonolysis of *trans*-3-hexene (initial mixing ratios: 8 ppm ozone, 15 ppm *trans*-3-hexene).

14088

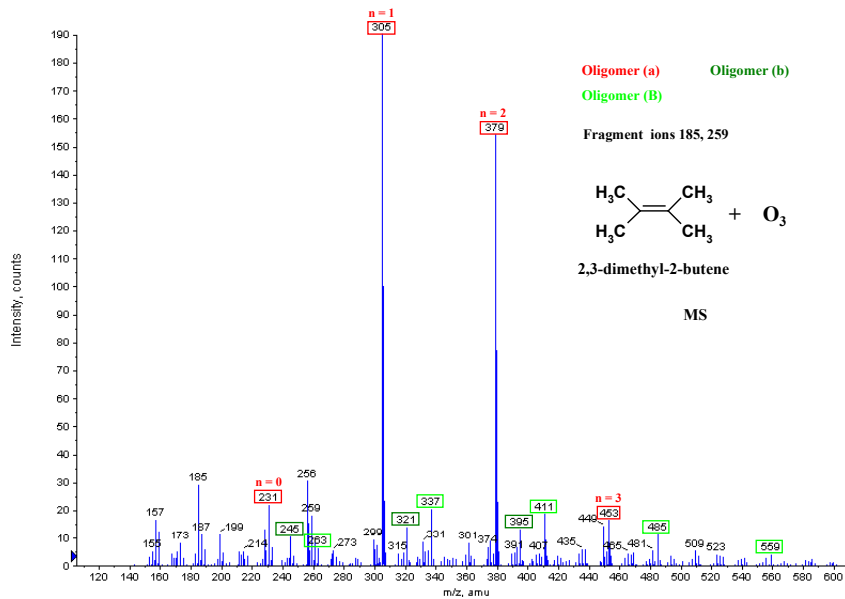


Fig. 2c. ESI(+)/MS-TOF mass spectrum of SOA formed during the gas phase ozonolysis of 2,3-dimethyl-2-butene (initial mixing ratios: 8 ppm ozone, 15 ppm 2,3-dimethyl-2-butene, 300 ppm cyclohexane).

14089

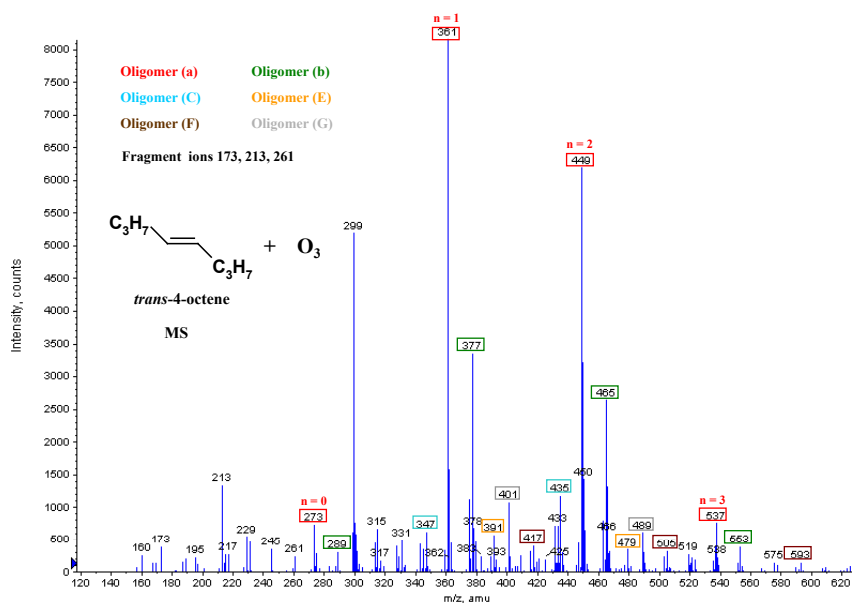


Fig. 2d. ESI(+)/MS-TOF mass spectrum of SOA formed during the gas phase ozonolysis of *trans*-4-octene (initial mixing ratios: 8 ppm ozone, 15 ppm *trans*-4-octene).

14090

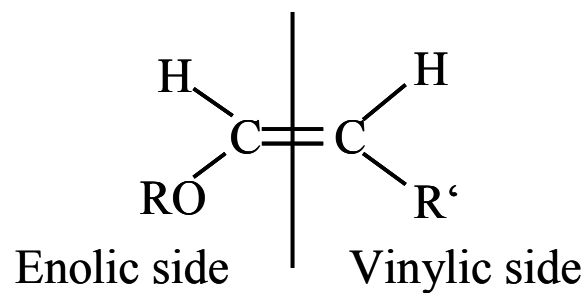


Fig. 3. Schematic structure of an enol ether.

14091

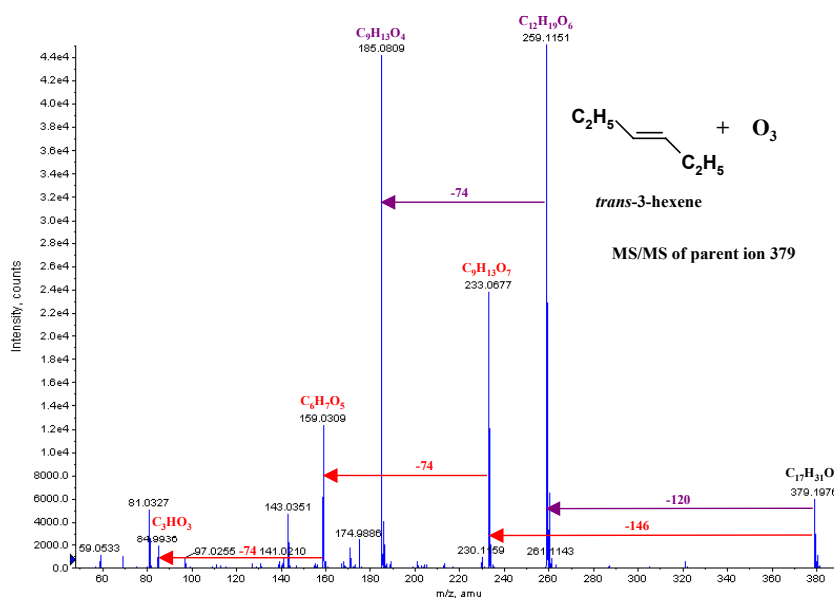


Fig. 4a. SOA formed during the gas phase ozonolysis of *trans*-3-hexene (initial mixing ratios: 8 ppm ozone, 15 ppm *trans*-3-hexene): ESI(+)/MS/MS-TOF spectrum of the parent ion 379 of oligomer (a).

14092

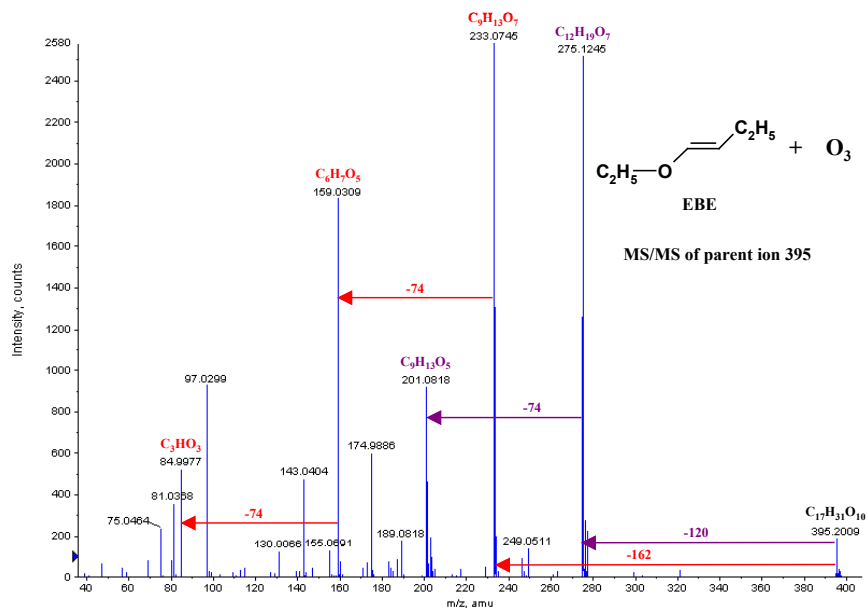


Fig. 4b. SOA formed during the gas phase ozonolysis of ethyl butenyl ether EBE (initial mixing ratios: 8 ppm ozone, 15 ppm EBE): ESI(+)/MS/MS-TOF spectrum of the parent ion 395 of oligomer (a).

14093

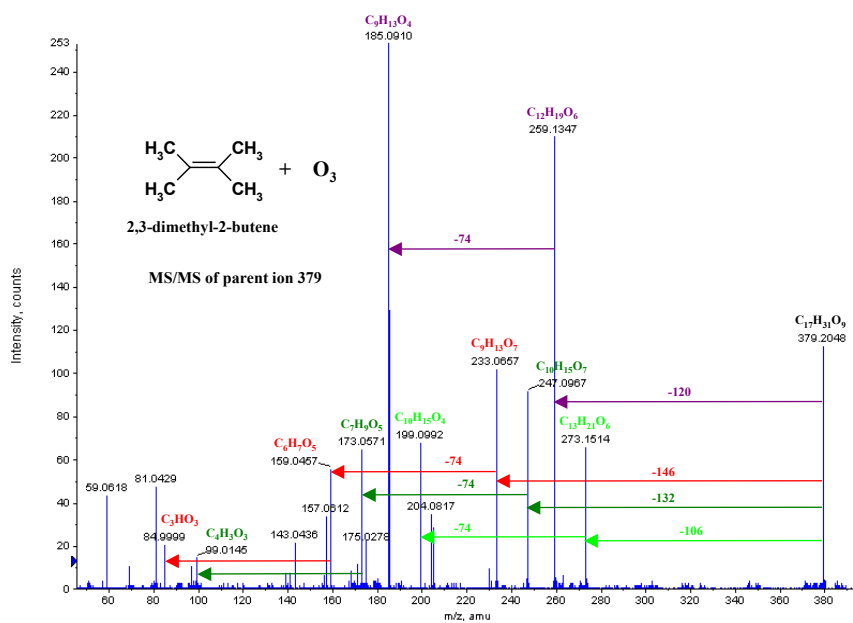


Fig. 4c. SOA formed during the gas phase ozonolysis of 2,3-dimethyl-2-butene (initial mixing ratios: 8 ppm ozone, 15 ppm 2,3-dimethyl-2-butene, 300 ppm cyclohexane): ESI(+)/MS/MS-TOF spectrum of the parent ion 379 of oligomer (a).

14094

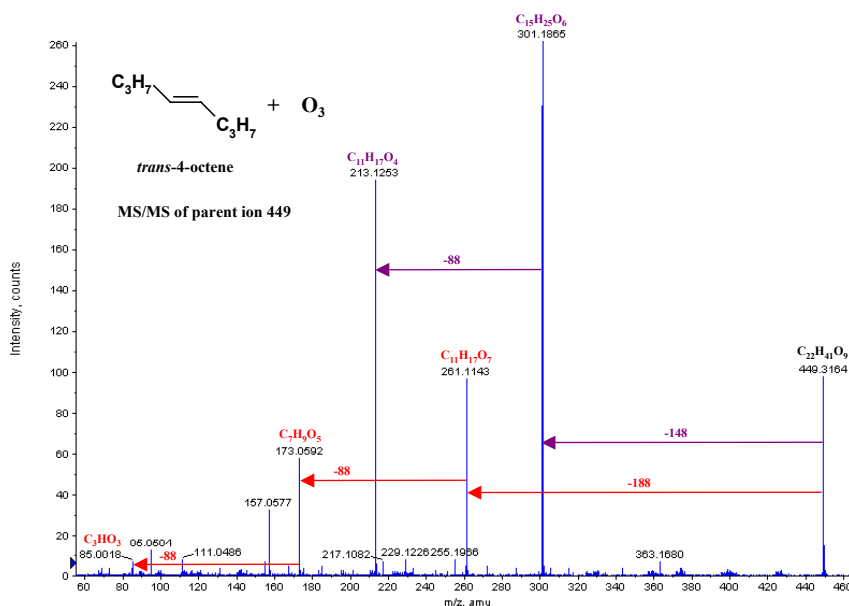


Fig. 4d. SOA formed during the gas phase ozonolysis of *trans*-4-octene (initial mixing ratios: 8 ppm ozone, 15 ppm *trans*-4-octene): ESI(+)/MS/MS-TOF spectrum of the parent ion 449 of oligomer (a).

14095

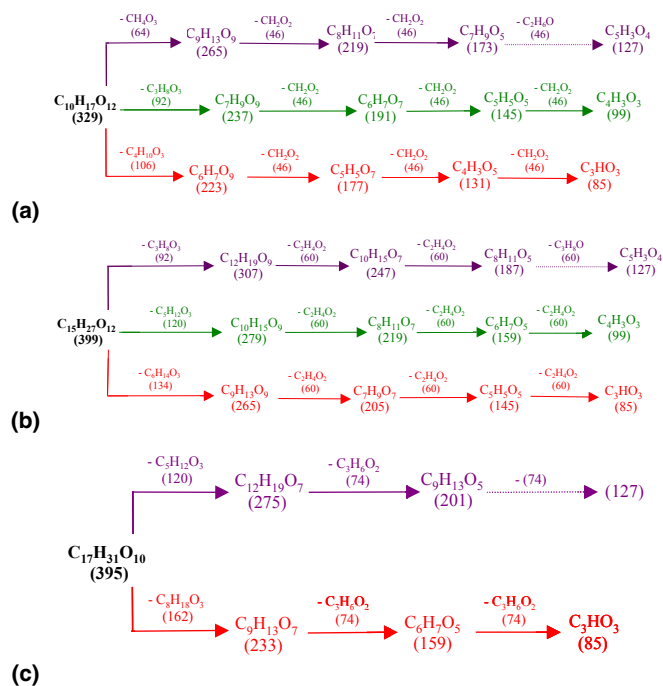


Fig. 5. Ozonolysis of enol ethers: Main fragmentation pathways of type (a) oligomer parent ions (a) Ozonolysis of ethyl vinyl ether (EVE, oligomer chain unit 46): Main fragmentation pathways of the type (a) oligomer parent ion 329 (Sadezky et al., 2006). (b) Ozonolysis of ethyl propenyl ether (EPE, oligomer chain unit 60): Main fragmentation pathways of the type (a) oligomer parent ion 399 (Sadezky et al., 2006). (c) Ozonolysis of ethyl butenyl ether (EBE, oligomer chain unit 74): Main fragmentation pathways of the type (a) oligomer parent ion 395.

14096

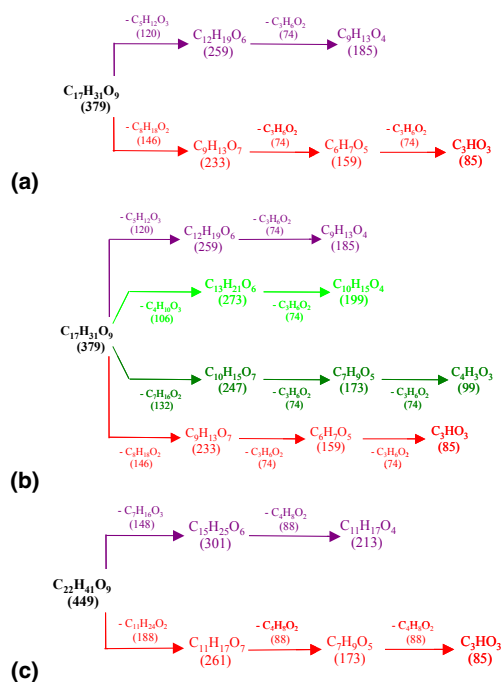


Fig. 6. Ozonolysis of symmetric alkenes: Main fragmentation pathways of type (a) oligomer parent ions. **(a)** Ozonolysis of *trans*-3-hexene (oligomer chain unit 74): Main fragmentation pathways of the type (a) oligomer parent ion 379. **(b)** Ozonolysis of 2,3-dimethyl-2-butene (oligomer chain unit 74): Main fragmentation pathways of the type (a) oligomer parent ion 379. **(c)** Ozonolysis of *trans*-4-octene (oligomer chain unit 88): Main fragmentation pathways of the type (a) oligomer parent ion 449.

14097

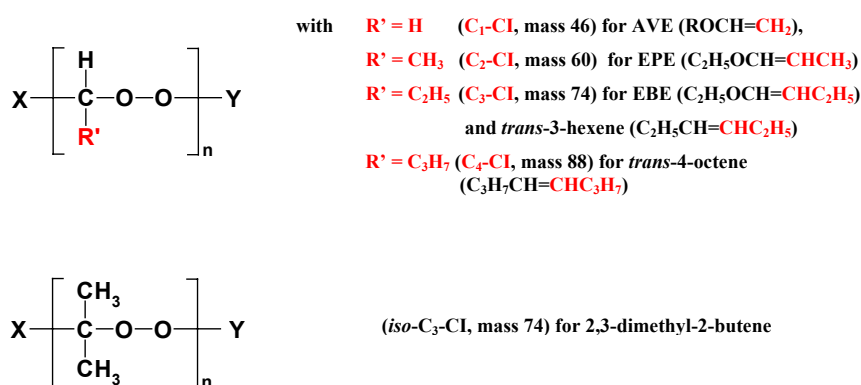


Fig. 7. Oligoperoxidic structure suggested for the oligomers formed during gas-phase ozonolysis of enol ethers and alkenes.

14098

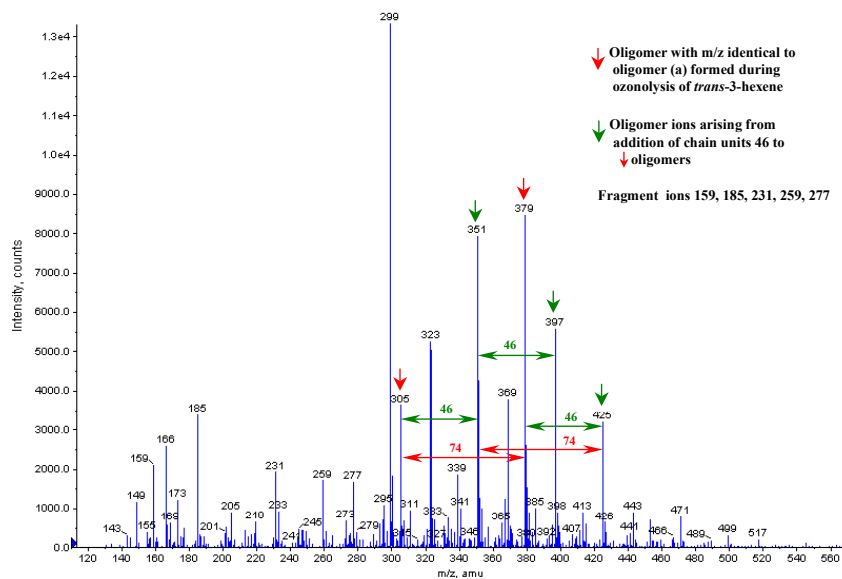


Fig. 8. ESI(+)/MS-TOF mass spectrum of SOA formed during simultaneous gas phase ozonolysis of *trans*-3-hexene and EVE (initial mixing ratios: 8 ppm ozone, 8 ppm EVE, 12 ppm *trans*-3-hexene).

14099

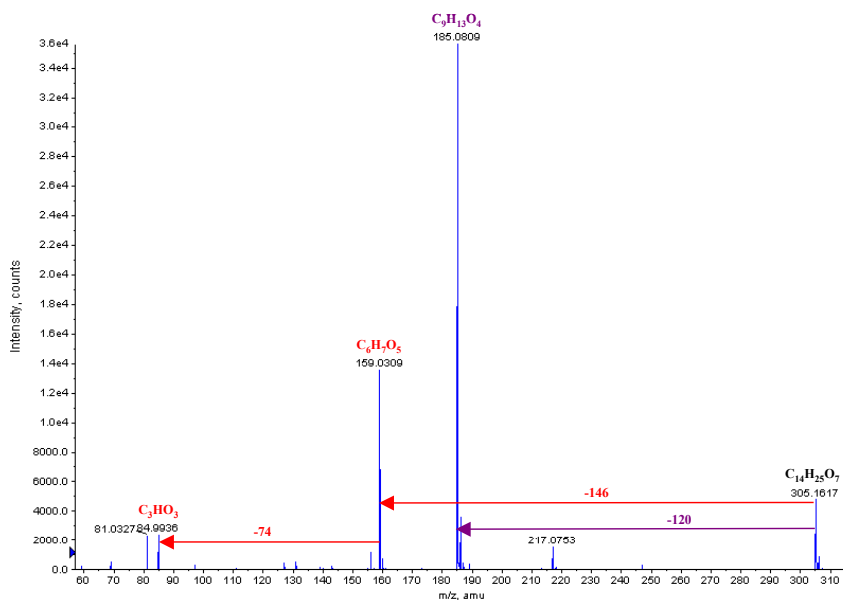


Fig. 9a. SOA formed during simultaneous gas phase ozonolysis of *trans*-3-hexene and EVE (initial mixing ratios: 8 ppm ozone, 8 ppm EVE, 12 ppm *trans*-3-hexene): ESI(+)/MS/MS-TOF spectrum of the parent ion 305.

14100

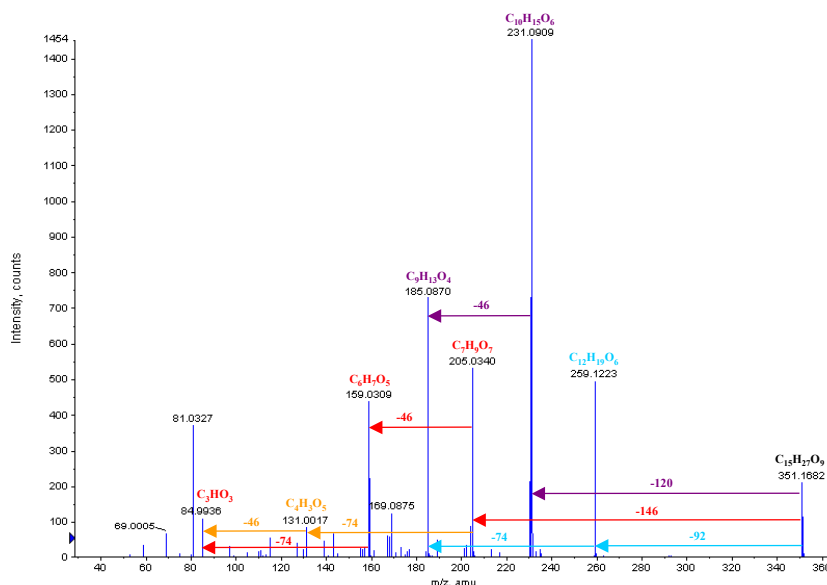


Fig. 9b. SOA formed during simultaneous gas phase ozonolysis of *trans*-3-hexene and EVE (initial mixing ratios: 8 ppm ozone, 8 ppm EVE, 12 ppm *trans*-3-hexene): ESI(+)/MS/MS-TOF spectrum of the parent ion 351.

14101

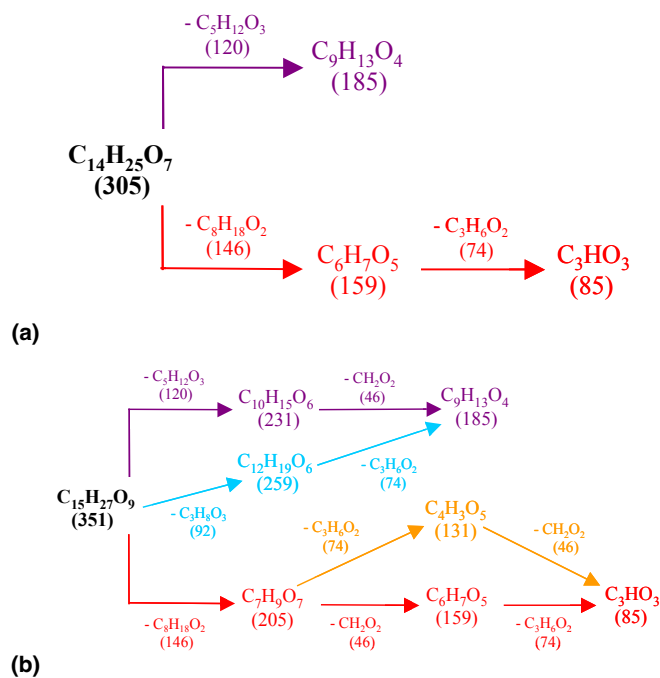


Fig. 10. Simultaneous gas phase ozonolysis of *trans*-3-hexene and EVE: Fragmentations of oligomer parent ions. (a) Main fragmentation pathways of the parent ion 305 (marked by a red arrow in Fig. 8) containing a single chain unit 74. (b) Main fragmentation pathways of the parent ion 351 (marked by a green arrow in Fig. 8) showing co-oligomerization of a chain unit 74 and a chain unit 46.

14102